




MISSOURI  
**S&T**

# CENTER FOR INFRASTRUCTURE ENGINEERING STUDIES



## **CLT AND AE METHODS OF IN-SITU LOAD TESTING: COMPARISON AND DEVELOPMENT OF EVALUATION CRITERIA**



**In-Situ Evaluation of Post-Tensioned  
Parking Garage,  
Kansas City, Missouri**

by

Paul H. Ziehl, Ph.D., P.E. and Nestore Galati, Ph.D.



**UTC  
R167**

**A University Transportation Center Program  
at Missouri University of Science & Technology**

## ***Disclaimer***

The contents of this report reflect the views of the author(s), who are responsible for the facts and the accuracy of information presented herein. This document is disseminated under the sponsorship of the Department of Transportation, University Transportation Centers Program and the Center for Infrastructure Engineering Studies UTC program at the University of Missouri - Rolla, in the interest of information exchange. The U.S. Government and Center for Infrastructure Engineering Studies assumes no liability for the contents or use thereof.

### Technical Report Documentation Page

1. Report No.  UTC R167	2. Government Accession No.	3. Recipient's Catalog No.		
4. Title and Subtitle  CLT AND AE METHODS OF IN-SITU LOAD TESTING: COMPARISON AND DEVELOPMENT OF EVALUATION CRITERIA In-Situ Evaluation of Post-Tensioned Parking Garage, Kansas City, Missouri		5. Report Date  February 2008		
		6. Performing Organization Code		
7. Author/s  Paul H. Ziehl, Ph.D., P.E. and Nestore Galati, Ph.D.		8. Performing Organization Report No.  00013027		
9. Performing Organization Name and Address  Center for Infrastructure Engineering Studies/UTC program Missouri University of Science & Technology 223 Engineering Research Lab Rolla, MO 65409		10. Work Unit No. (TRAIS)		
		11. Contract or Grant No.  DTRS98-G-0021		
12. Sponsoring Organization Name and Address  U.S. Department of Transportation Research and Special Programs Administration 400 7 <sup>th</sup> Street, SW Washington, DC 20590-0001		13. Type of Report and Period Covered  Final		
		14. Sponsoring Agency Code		
15. Supplementary Notes				
16. Abstract  The objective of the proposed research project is to compare the results of two recently introduced nondestructive load test methods to the existing 24-hour load test method described in Chapter 20 of ACI 318-05. The two new methods of nondestructive evaluation are the Cyclic Load Test (CLT) and Acoustic Emission (AE) methods. Each method offers advantages over the 24-hour load test method and each is particularly well suited to different aspects of structural evaluation. The focus of the research effort is an existing reinforced concrete (RC) building in Kansas City, Missouri. This building provides an ideal real world test bed for comparison between the three different methods of in-situ evaluation (24-hour, CLT, and AE methods).  Preliminary results from this experimental campaign will form the basis for future research related to the appropriateness of each method and the understanding of each method on a more fundamental basis. The research proposed will provide the initial data that is necessary for the successful pursuit of larger funds from international agencies. The proposed seed monies will be used as the basis for follow-up grants that will be written to the National Science Foundation, the European Community, the Engineering and Physical Sciences Research Council (EPSRC) and other agencies to test full-scale structures in the laboratory and in the field in order to validate the changes proposed by ACI 437: Strength Evaluation of Existing Concrete Buildings and to provide sufficient engineering evidence that is currently missing.				
17. Key Words  Crack Propagation, Structural Assessment, Inspection and Mitigation Strategies, Risk Management, Cyclic Load Testing, 24-h Testing, Acoustic Emission		18. Distribution Statement  No restrictions. This document is available to the public through the National Technical Information Service, Springfield, Virginia 22161.		
19. Security Classification (of this report)  unclassified		20. Security Classification (of this page)  unclassified	21. No. Of Pages  43	22. Price

**CLT AND AE METHODS OF IN-SITU LOAD TESTING:  
COMPARISON AND DEVELOPMENT OF EVALUATION  
CRITERIA**

**In-Situ Evaluation of Post-Tensioned Parking Garage,  
Kansas City, Missouri**

SUBMITTED TO THE CONCRETE RESEARCH COUNCIL

CRC research proposal no. 2006-42

written by

**Paul H. Ziehl, Ph.D., P.E. – University of South Carolina, USA**

**Nestore Galati, Ph.D. – University of Missouri-Rolla, USA**

*Contact information:*  
University of South Carolina  
Department of Civil and Environmental Engineering  
300 Main Street  
Columbia, SC 29208  
Dr. Paul Ziehl, [ziehl@engr.sc.edu](mailto:ziehl@engr.sc.edu), 803 777 0671

# TABLE OF CONTENTS

1.	INTRODUCTION .....	1
1.1	Objectives of the Investigation .....	1
1.2	Technical Focus of the Investigation .....	1
1.3	Description of the Building.....	1
1.4	Simulation of Distributed Loading .....	3
1.5	Load Intensity .....	3
1.6	Load Configuration.....	4
1.7	Load Test Protocols and Acceptance Criteria.....	5
1.7.1	24 h Load Test: ACI 318-05 Chapter 20 .....	5
1.7.2	Cyclic Load Test: ACI 437 .....	5
1.7.3	Acoustic Emission .....	9
2.	PRELIMINARY INVESTIGATIONS .....	14
2.1	Structural Geometry.....	14
2.2	Material Characteristics .....	14
2.3	Structural Capacity .....	14
2.4	Determination of Equivalent Loads .....	15
3.	DESCRIPTION OF THE LOAD TEST .....	17
3.1	Testing Apparatus .....	17
3.2	Load Test Configurations .....	19
3.3	Deflection Measurement.....	20
4.	TESTING PROCEDURE .....	23
5.	TEST RESULTS AND DISCUSSION .....	25
5.1	Cyclic Load Test (with Simulated Shear Collar).....	25
5.2	Acoustic Emission (with Simulated Shear Collar) .....	26
5.3	24 h Load Test (with Simulated Shear Collar) .....	28
5.4	Cyclic Load Test (with CFRP Strengthening).....	29
5.5	Acoustic Emission (with CFRP Strengthening) .....	33
6.	CONCLUSIONS.....	36
7.	ACKNOWLEDGEMENTS.....	38
8.	REFERENCES .....	39

# 1 INTRODUCTION

In April of 2006 the Concrete Research Council sponsored a grant in the amount of \$9,550 for a project entitled: *CLT and AE Methods of In-Situ Load Testing: Comparison and Development of Evaluation Criteria*. This grant provided assistance with travel to the site of a post-tensioned parking garage structure in Kansas City, Missouri for purposes of collecting necessary data during load testing. This report describes the building itself, the method of load application, and the in-situ evaluation criteria. A supplemental report will be submitted at a later date related to comparison of in-situ evaluation criteria for the case of full-scale AASHTO type III girders in a laboratory environment.

## 1.1 Objectives of the Investigation

The objectives of this investigation were:

- To collect the initial data that is necessary for the successful pursuit of larger funds from national and international agencies.
- To further the development of in-situ evaluation methods for RC structures

In regard to the first objective, a proposal has been developed and submitted to the National Science Foundation.

In regard to the second objective, based on the data collected during testing two journal articles are in preparation and presentations have been given to the ACI Concrete Research Council, ACI Committee 437 (Strength Evaluation of Existing Concrete Buildings), and to a general audience at the 2006 ACI Fall Convention in Denver, Colorado.

## 1.2 Technical Focus of the Investigation

The technical focus of this investigation was the comparison of different evaluation methods for RC structures. In particular, it was desired to compare the evaluation criteria of two recently introduced in-situ load test methods to the existing 24-hour load test method described in Chapter 20 of ACI 318-05. The more recently proposed evaluation methods are the Cyclic Load Test (CLT) and Acoustic Emission (AE) methods. Each of the more recent methods offers advantages over the 24-hour load test method.

## 1.3 Description of the Building

The garage under investigation is a free-standing, four-story, open parking structures constructed of cast-in-place, post-tensioned, two-way concrete flat plates. A flat plate is a structural system that consists of slabs without beams or thickened slabs (drop panels) near columns. The slabs are internally reinforced with unbonded post-tensioned tendons and mild steel reinforcement. In one direction, the post-tensioning tendons are approximately uniformly spaced (uniform tendons). The uniform tendons are mostly oriented parallel to the shorter building plan dimension (east-west). In the direction perpendicular to the uniform tendon direction, the post-

tensioning tendons are placed adjacent to one another in bands that are in line with and extend through the columns (banded tendons). There are no post-tensioning tendons between and parallel to the bands of tendons on the column lines. The slabs are supported by circular cast-in-place concrete columns with column capitals at the top of some columns.

The parking deck slabs exhibited varying degrees of cracking and deterioration, which led the owner of the parking garage to retain Simpson Gumpertz & Heger Inc. (SGH) to review the gravity-load carrying strength of the suspended parking deck slabs, to assess the condition of the suspended parking deck slabs, to identify the causes of cracks and deterioration, and to identify remedial work necessary to repair existing deterioration and to correct structural and durability deficiencies of the suspended parking deck slabs.

SGH review considered as-built reinforcement placement and slab thicknesses, prepared construction documents for the structural strengthening, concrete repair, and concrete protection of the suspended post-tensioned concrete parking deck slabs of the parking garage. The garage had many areas of the slabs where low tendon and mild steel placement, mainly in the uniform tendon direction, resulted in inadequate flexural strength and shear/flexure transfer at column/slab intersections. SGH selected two representative areas of the slabs to be load tested and their performance to be evaluated before and after strengthening with an externally bonded carbon fiber reinforced polymer (CFRP) composite system.

This report describes the load tests performed on a representative area of the garage as shown in Figure 1.1. Two tests were performed comparing the performance of different strengthening techniques (i.e. simulated shear collar and CFRP strengthening), and following different protocols. The aim of the load tests was to assess the structural performance of the floor system to negative moments in correspondence of selected columns as highlighted in Figure 1.1.

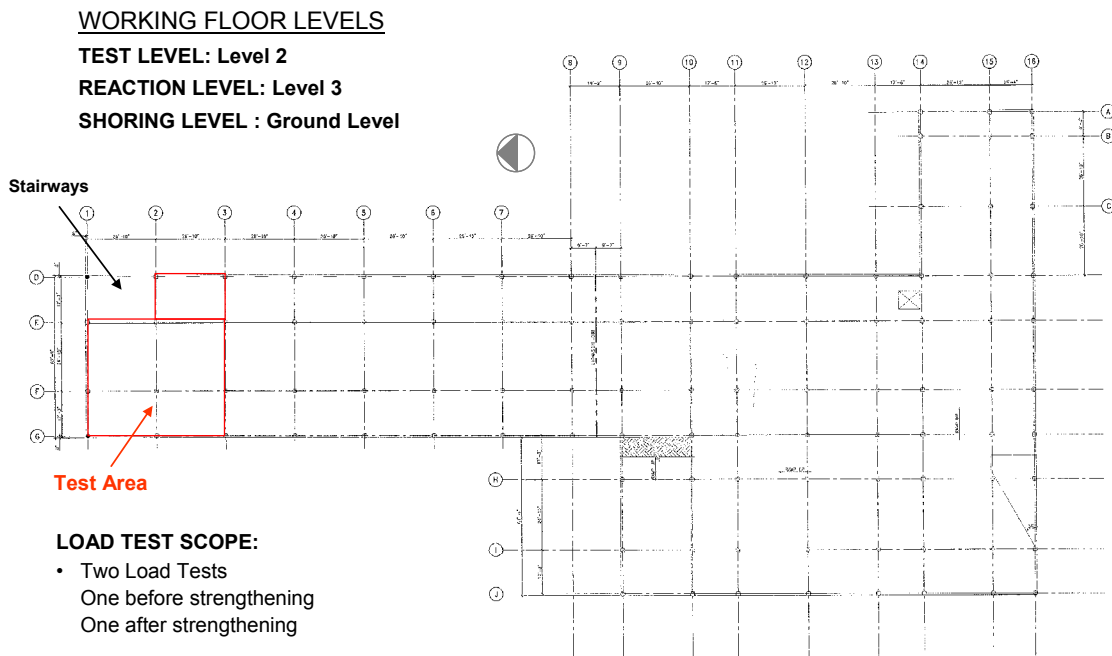


Figure 1.1: Load Test Area: Column F2, Level 2 Uniform Tendons Direction

The load test procedure involved applying concentrated loads to the structural floor components at pre-determined locations. The response of the slab in the vicinity of the applied loads was monitored and used to evaluate its performance.

#### 1.4 Simulation of Distributed Loading

The design loads were simulated by means of hydraulic jacks that are relatively easy to install and control. For the structure under investigation, the design live load is uniformly-distributed downward pressure acting over the entire surface of the slab. Since the load from the hydraulic jacks is concentrated, the effects of the design load can only be simulated on a relatively small portion of the slab. In the unlikely event that permanent damage be inflicted to the slab (such as yielding of the steel reinforcement), this damage would be limited to the localized area of loading with little consequences on the performance of the overall system.

#### 1.5 Load Intensity

Three load intensity levels were used. The recently published ACI 437.1R-07 [ACI 437, 2007] recommends that the load intensity as provided in Chapter 20 of 318-05 [ACI, 2005] be re-defined as follows. Since only part of the structure's suspect portions is to be load tested, and elements to be tested are indeterminate, the test load magnitude, TLM, (including dead load already in place) was chosen to be not be less than

$$\text{TLM} = 1.3 (D_w + D_s) \quad (1)$$

or

$$\text{TLM} = 1.0 D_w + 1.1 D_s + 1.6L + 0.5 (L_r \text{ or } S) \quad (2)$$

or

$$\text{TLM} = 1.0 D_w + 1.1 D_s + 1.6 (L_r \text{ or } S) + 1.0 L \quad (3)$$

where  $D_w$  is the dead load due to the self-weight;  $D_s$  is the superimposed dead load;  $L$  is the live loads produced by the use and occupancy of the building not including construction or environmental loads such as wind load, snow load, rain load, earthquake load, flood load, or superimposed dead loads;  $L_r$  is the roof live loads produced during maintenance by workers, equipment, and materials or during the life of the structure by moveable objects such as planters and people; and  $S$  is the snow load.

For the building under investigation, the superimposed dead load is equal to zero, as are the snow and roof live loads; therefore, the test load magnitude is given by

$$\text{TLM} = 1.0 D_w + 1.6L \quad (4)$$



The first objective of the load test was, therefore, to determine the reaction of the floor system to negative moments in connection with selected columns by using the load combination given by Eq. (4).

Additionally, as requested by SGH, all the test areas were also subjected to the load combination shown in Eq. (5), being the load combination under consideration by the ACI 318 committee at the time of the test.

$$TLM = 1.15D + 1.5L \quad (5)$$

For this structure, such load combination ( $1.15D + 1.5L = 154.3 \text{ psf}$ ) is very close to  $0.85(1.4D + 1.7L) = 155.4 \text{ psf}$  prescribed by ACI 318-05 Chapter 20.

Finally, for the strengthened area using CFRP laminates bonded at the negative moments region, the design load level given in Eq. (6) was also applied to the structure.

$$TLM = 1.2 D + 1.6L \quad (6)$$

### 1.6 Load Configuration

The load was applied at four points distributed around the column of interest as shown in Figure 1.2. The intensity of the applied load at each point was determined, so the same effect in terms of negative moment resulting from the factored, uniformly-distributed load defined by Equations (4) to (6) could be produced.

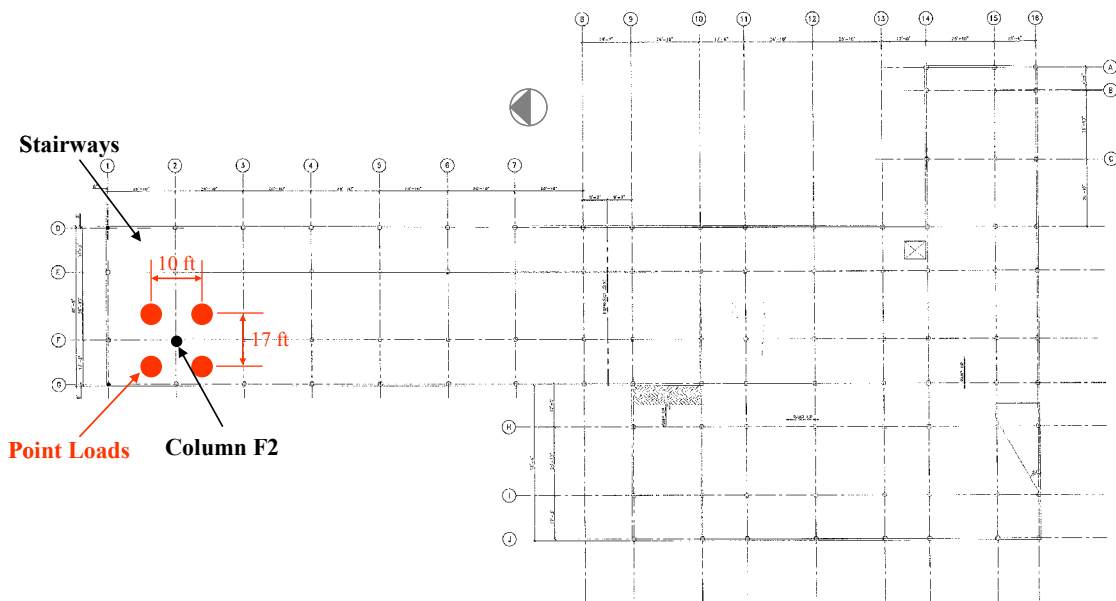


Figure 1.2: Loading Points

## 1.7 Load Test Protocols and Evaluation Criteria

The following two sections describe the load test protocols and acceptance criteria according to ACI 318 (24h load test), ACI 437 (Cyclic Load Test) and Acoustic Emission.

### 1.7.1 24 h Load Test: ACI 318-05 Chapter 20

In-situ load testing adopted by ACI 318-05 Ch. 20 is based on a relatively long-term duration of loading. Once the structure is adequately instrumented, at the locations where the maximum response is expected, initial values of each instrument shall be recorded not more than one hour before the application of the first load increment.

After the test is started, the load must be applied in not less than 4 approximately equal increments. If the measurements are not recorded continuously, a set of response readings should be registered at each of the 4 load increments till reaching the total test load and also registered after the test load has been applied on the structure for at least 24 hours. Once the aforementioned readings have been taken, the test load must be removed immediately, and a set of final readings must be made 24 hours after the test load is removed.

The evaluation of the structure is based on two different sets of acceptance criteria to certify whether the member tested has passed the load test or not. First, a set of visual parameters (*e.g.*, no spalling or crushing of compressed concrete and evidence of excessive deflections) that would obviously be incompatible with the safety requirements of the structure should be evaluated. Secondly, the measured maximum deflections shall satisfy one of the following two equations:

$$\Delta_{max} = \frac{l_i^2}{20,000h} \quad (7)$$

$$\Delta_{rmax} \leq \frac{\Delta_{max}}{4} \quad (8)$$

If the measured maximum and residual deflections do not satisfy Equation (7) or (8), the load test may be repeated, but not earlier than 72 hours after the removal of the first test load as specified in ACI 318-05 Section 20.5.2.

Even though this load test protocol has been used and has become part of engineering practice, no rationale or experimental evidence seems to substantiate its validity. Time constraints and costs can make the use of this test prohibitive.

### 1.7.2 Cyclic Load Test: ACI 437

The main difference between the protocol of the cyclic load test and the 24-hour load test is that the load is applied in cycles by using hydraulic jacks, which are easily controlled by hand or electric pumps, assuring that the load could be removed in matter of seconds. Increasing both loading and unloading cycles up to a predetermined maximum load will allow the engineer a safer real-time assessment of member characteristics (*e.g.*, linearity and repeatability of response,

as well as permanency of deformations). The duration of the cyclic load is considerably reduced from that of the 24-hour load test.

The preliminary steps in planning the load test (including preliminary investigation, structural analysis, and load definition) are the same as for the 24-hour load test. The main difference between these two protocols relies on the procedure by which the load is applied.

The procedure of a cyclic load test consists of the application of concentrated loads in a quasi-static manner to the structural member, in at least six loading/unloading cycles. The number of cycles and the number of steps, as described in the following, should be considered the minimum requirement:

1. Benchmark: The initial reading of the instrumentation is taken no more than 30 minutes before beginning the load test and any load being applied. The benchmark is shown in Figure as the constant line beginning at time zero and indicating no load.
2. Cycle A: The first load cycle consists of 5 load steps, each increased by no more than 10 percent of the total test load expected in the cyclic load test. The load is increased in steps until the service level of the member is reached, but should not surpass more than 50 percent of the total test load, as shown in Figure . The maximum load level for the cycle should be maintained until the structural response parameters have stabilized. During each unloading phase, a minimum load ( $P_{min}$ ) of at least 10 percent of the total test load should be maintained to keep the test devices engaged.
3. Cycle B: A repeat of Cycle A that provides a check of the repeatability of the structural response parameters obtained in the first cycle.
4. Cycles C and D: Load Cycles C and D are identical and achieve a maximum load level that is approximately half way between the maximum load level achieved in Cycles A and B and 100 percent of the total test load. The loading procedure is similar to that of Load Cycles A and B.
5. Cycles E and F: The fifth and sixth load cycles, E and F, respectively, should be identical, and they should reach the total test load, as shown in Figure .
6. Final Cycle: At the conclusion of Cycle F, the test load should be decreased to zero, as shown in Figure . A final reading should be taken no sooner than two minutes after the total test load (not including the equipment used to apply the load) has been removed.

Figure illustrates a schematic load versus deflection curve derived from the six cycles mentioned above.

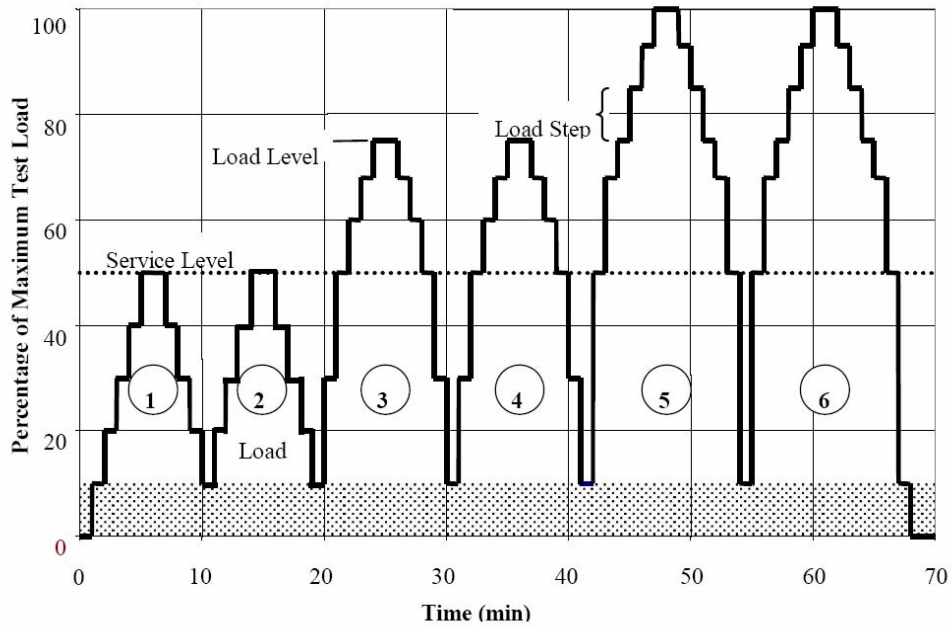


Figure 1.3: Load Steps and Cycles for a Cyclic Load Test

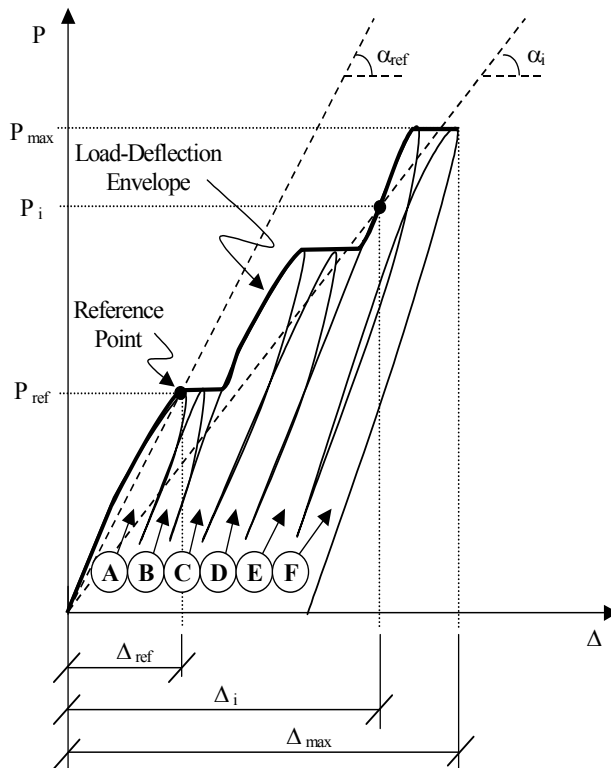


Figure 1.4: Schematic Load Versus Deflection Curve for Six Cycles

Similar to the 24-hour load test, the Cyclic Load Test has acceptance criteria to be checked during and after the load test to establish whether the member tested has passed the proof test.

The three parameters that have been established to analyze the behavior of a tested structure are the following, and all are related to the response of the structure in terms of displacement:

1. Repeatability: Represents the behavior of the structure during two identical loading cycles. By measuring the repeatability of deflections, one is not only monitoring the structure's behavior, but is also gaining assurance that the data collected during the test is consistent. Repeatability is calculated according to the following equation referring to Figure 1.5:

$$\text{Repeatability} = \frac{\Delta_{max}^B - \Delta_r^B}{\Delta_{max}^A - \Delta_r^A} \times 100\% \geq 95\% \quad (9)$$

Experience [Mettemeyer, 1999] has shown that a repeatability of greater than 95 percent is satisfactory.

2. Permanency: Represents the amount of permanent change displayed by any structural response parameter during the second of two identical load cycles. Permanency should be less than 10 percent (Mettemeyer, 1999) and is computed by the following equation referring to Figure 1.5 **Figure** (e.g., during cycle B):

$$\text{Permanency} = \frac{\Delta_r^B}{\Delta_{max}^B} \times 100\% \leq 10\% \quad (10)$$

If the level of permanency of the second of two repeated cycles is higher than the aforementioned 10 percent, it may be an indication that the repeated loading has damaged the structural member further and that nonlinear effects are taking place.

3. Deviation from Linearity: Represents the measure of the nonlinear behavior of a member being tested. As the member becomes increasingly more damaged, its behavior may become more nonlinear, and its deviation from linearity may increase.

To define deviation from linearity, linearity itself should first be defined. Linearity is the ratio of the slopes of two secant lines intersecting the load-deflection envelope. The load deflection envelope is the curve constructed by connecting the points corresponding to only those loads greater than or equal to any previously applied loads, as shown in Figure 1.5 **Figure**. The linearity of any point  $i$  on the load-deflection envelope is the percent ratio of the slope of that point's secant line ( $\tan \alpha_i$ ) to the slope of the reference secant line ( $\tan \alpha_{ref}$ ), as expressed by Equation (6):

$$\text{Linearity} = \frac{\tan \alpha_i}{\tan \alpha_{ref}} \times 100\% \quad (11)$$

The deviation from linearity of any point on the load-deflection envelope is the compliment of the linearity of that point, as given in the following:

$$\text{Deviation from Linearity} = 100\% - \text{Linearity} \leq 25\% \quad (12)$$

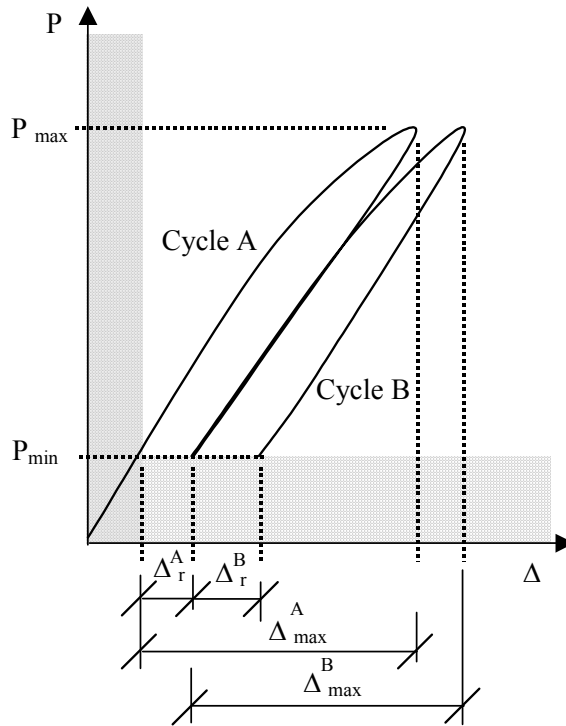


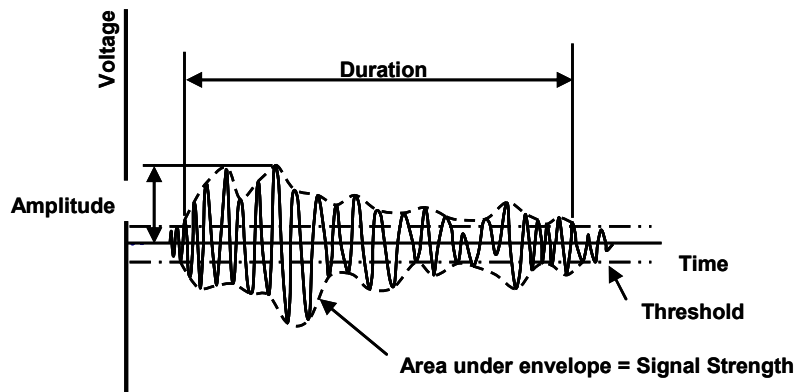
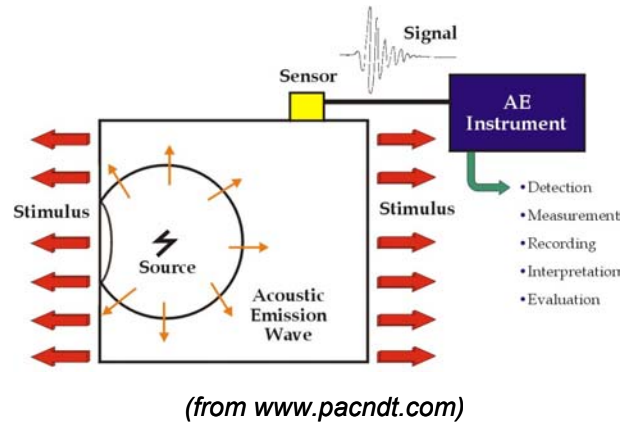
Figure 1.5: Schematic Load Versus Deflection Curve for two Cycles

Once the level of load corresponding to the reference load has been achieved, deviation from linearity should be monitored until the conclusion of the cyclic load test. Experience [Mettemeyer, 1999] has shown that the values of deviation from linearity, as defined above, are less than 25 percent. Deviation from linearity may not be useful when testing a member that is expected to behave in an elastic manner; for such a member, its repeatability and permanency, as previously defined, may be better indicators of damage in the tested structure.

### 1.7.3 Acoustic Emission Evaluation

Acoustic emission has been used in the past for evaluation of reinforced concrete specimens [Hearn and Shield, 1997, Ohtsu et al., 2002, Ridge and Ziehl, 2006, and Colombo et al., 2005]. It has recently been applied in the field for the evaluation a hybrid FRP/reinforced concrete bridge structure [Ziehl et al., 2005a and b] and for a prestressed concrete bridge during the passage of an extreme overload [Ziehl, 2003a]. Acoustic emission evaluation has been used as an in-situ evaluation tool in the FRP vessel industry for over 20 years and many of the evaluation techniques for reinforced concrete borrow from the codes and standards developed for that industry [ASME, 2004a and b]. For civil infrastructure codes do not currently address assessment by the acoustic emission method, however, a standard procedure has been developed [JSNDI, 2000].

Acoustic emission can be defined as transient elastic waves that are produced by a sudden release of energy such as that due to crack growth. A schematic of the instrumentation and an acoustic emission hit are shown in Figure 1.6. Because a release of energy is necessary for the acoustic emission method some form of loading is required. Furthermore, load and load history are important to the evaluation and most of the criteria are related to acoustic emission (AE) that is recorded during the reloading phase. Terminology related to acoustic emission examination can be found in ASTM [ASTM, 2006]. Many methods have been proposed for AE evaluation, some of which are described below.



**Acoustic emission hit**

Figure 1.6: Schematic of Acoustic Emission data acquisition system and AE hit

**Cumulative signal strength ratio**

Previous studies by Ridge [Ridge and Ziehl, 2006] have indicated that the acoustic emission energy that is generated during reloading when compared to that generated during initial loading can be useful as an indicator of damage. Cumulative signal strength was used in the studies by Ridge because this parameter is related to the energy released during loading. Ridge conducted experiments on medium-scale reinforced concrete beam specimens that had been strengthened

with CFRP materials. The experiments focused on flexural behavior and the AE parameter of signal strength was used for purposes of comparison.

For the tests described in this report, a similar approach to evaluation was taken for each of the loadsets. Because the peak load for each of the cycles in all loadsets was similar it was not feasible to focus on emissions during the load hold periods. Rather, cumulative signal strength was plotted versus time for each cycle of each loadset (see Figure 1.7) during the loading phase. The value of cumulative signal strength during each reloading cycle was then compared to that for the initial loading cycle and expressed as a percentage. In this figure the pink area represents data that was filtered due to persons walking in the loading area which lead to non-genuine emission. The CSS ratio can be expressed as:

$$CSS \text{ ratio during loading} = (CSS \text{ during initial loading} / CSS \text{ during reloading}) * 100\%$$

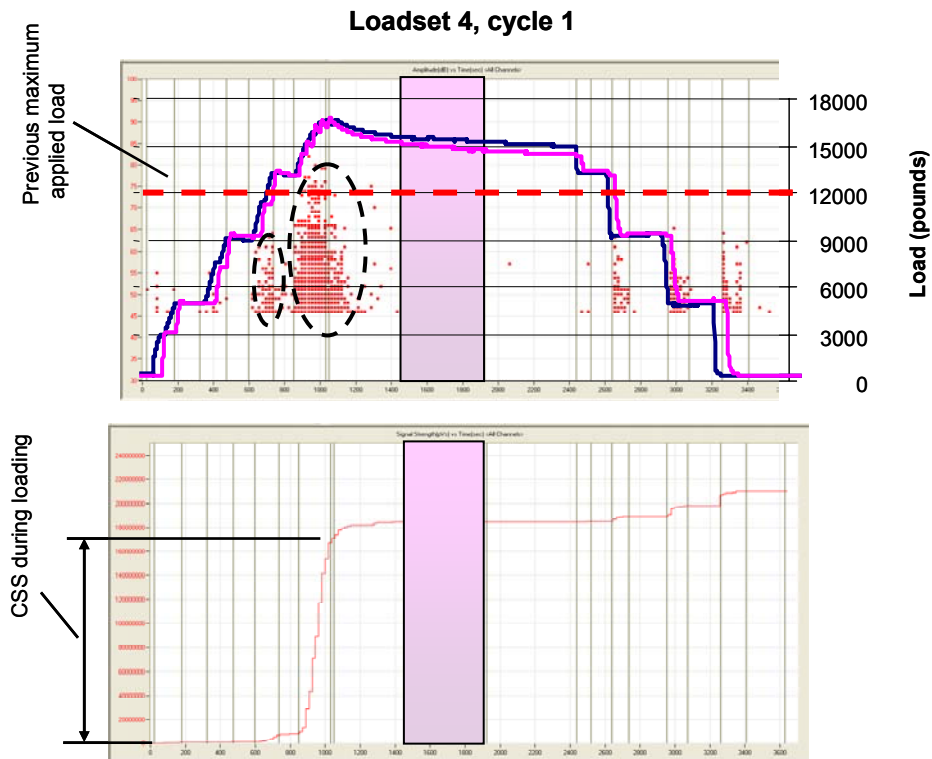


Figure 1.7: AE data from Loadset 4, Cycle 1 (after CFRP Strengthening)



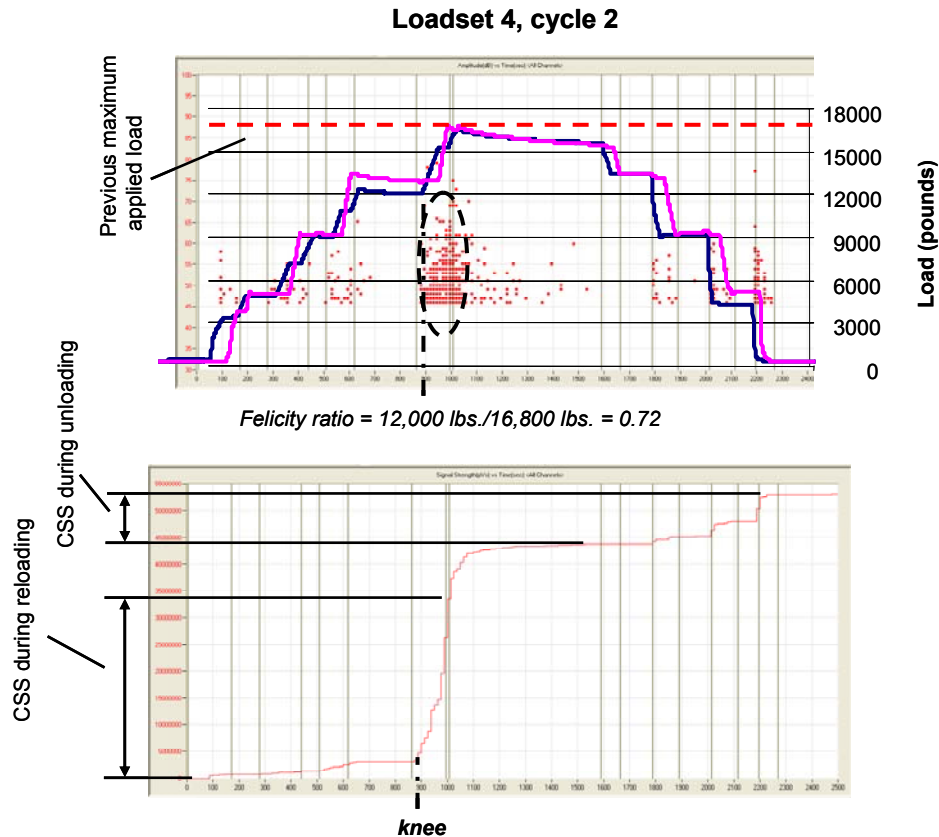


Figure 1.8: AE data from Loadset 4, Cycle 2 (after CFRP Strengthening)

### Felicity ratio

The Felicity effect is essentially the inverse of the Kaiser effect. While the Kaiser effect is the lack of AE activity during reloading to the previously applied maximum load level, the Felicity effect is the presence of AE activity during the reloading period. When the Kaiser effect is present, the Felicity ratio has a value of 1.0. As damage is increased the Felicity ratio drops below 1.0 and generally decreases as damage is increased. In publications related to reinforced concrete the Felicity ratio is often referred to as the ‘load ratio’ or the ‘concrete beam integrity ratio’ [Ohtsu et al., 2002].

One difficulty with quantifying the Felicity effect (and calculating the associated Felicity ratio) is the determination of the onset of significant AE activity. If any increase in AE activity during reloading is used to define the Felicity effect then very low Felicity ratios can be calculated that are not representative of the actual behavior of the structure. In codes related to FRP pressure vessels this has been addressed through the use of historic index to determine the onset of significant acoustic emission activity. For this report, visual inspection of the cumulative signal strength versus time curve was used to determine the onset of significant acoustic emission. Felicity ratios were then determined as follows:

$$\text{Felicity ratio} = (\text{load at onset of significant AE during reloading}) / (\text{previous maximum load})$$

### **Calm ratio versus load ratio (Felicity ratio)**

A third assessment technique that has been proposed is a comparison of ‘calm ratio’ versus ‘load ratio’. Load ratio is identical to Felicity ratio as previously defined. Calm ratio [Ohtsu et al., 2004] compares the AE activity during loading to that during unloading. For this investigation it was defined as:

$$\text{Calm ratio} = (\text{cumulative signal strength during unloading} / \text{cumulative signal strength during previous maximum loading cycle})$$

For this report the calm ratio was calculated for the reloading cycles only.

### **Location Plots**

While source location is not the focus of this investigation, location plots are easily generated if the wavespeed of the material is known. For this report, wavespeed was determined with pencil lead breaks on-site and the program 2D-loc (for two dimensional location) was used to determine the source of the AE activity.

## 2 Preliminary Investigations

The following summarizes the preliminary assessment of the structure and the sources for the information used in designing the load tests. Assumptions made in the design of the load tests were checked by SGH.

### 2.1 Structural Geometry

The structural geometry including column locations and member sizes were determined from the engineering drawings supplied by SGH.

The structural floor is a two-way, post-tensioned (PT) slab, supported by circular and square columns provided with capital to avoid punching shear failure. The concrete slab was mostly 6.5 in thick.

### 2.2 Material Characteristics

The material characteristics were provided by SGH. The specifications indicated a nominal concrete strength of 4000 psi, minimum yield strength of 60 ksi for the mild reinforcement of the steel, and an effective stress in the tendons from a prestress of 176 ksi. The tendons consisted of low-relaxation, 270-ksi, 7-wire strands.

### 2.3 Structural Capacity

The design loading conditions were derived from information given by SGH.

- The structural review is based on the gravity loads prescribed by the 2003 International Building Code (IBC), which is the code currently adopted by the City of Kansas City.
- The factored uniform load for design/review of lower levels is  $1.2D_w + 1.6L$ .
- The Dead Load is the self-weight of the structure (6.5 in slab) plus an additional 6 psf to account for as-built conditions of slab thickness.
- The Live Load is 40 psf for passenger vehicle garages.

The negative bending moment capacity and shear capacity of the area under investigation were obtained from SGH.

Table 2.1 provides a summary of the values of moment capacity for the structural members of interest and also provides the specific objective of each load test as requested by SGH. Please note that the shear/flexural transfer capacity at column slab intersections is not adequate; therefore, shoring posts to simulate the presence of shear collars were used for the tests on the unstrengthened areas. Since SGH estimated that the shear collars needed to prevent shear failure

must have a diameter of 4 ft, the shoring posts should cover a minimum area around the columns of 8 ft<sup>2</sup>.

Table 2.1: Moment Demand & Capacity of Structural Members

Location	Test Label	Condition	$M_u$ [kip-ft]	$\phi M_n$ [kip-ft]	Objective
Garage A, Level 2, Column F-2. Typical 26 ft-10 in wide, three-bay frame, Uniform tendon direction	GA-U1	Shear Collar	189	143 <sup>(1)</sup>	Assess performance of slab with simulated shear collar.
	GA-U1-C	Shear Collar			Evaluate crack widths at service Compare ACI 437 to ACI 318 procedure
	GA-U1-S	CFRP Strengthened		189 <sup>(2)</sup>	Assess performance of slab after strengthening

<sup>(1)</sup> Nominal capacity in correspondence of the capital. The nominal capacity at the shear collar location was not provided. <sup>(2)</sup> Minimum capacity to be achieved by strengthening.

## 2.4 Determination of Equivalent Loads

Numerical models were implemented to determine the magnitude of the concentrated point loads that produce the same positive bending moment of the factored uniformly distributed loads (UDL) at the critical test section.

A two-dimensional model of the main structural elements combined with a plate element representing the slab was used. The model consisted of one-dimensional beam elements representing columns. A fine mesh of plate elements was created to represent the floor systems. The FEM model was implemented in commercial FEM software, SAP2000 (see Figure 2.1).

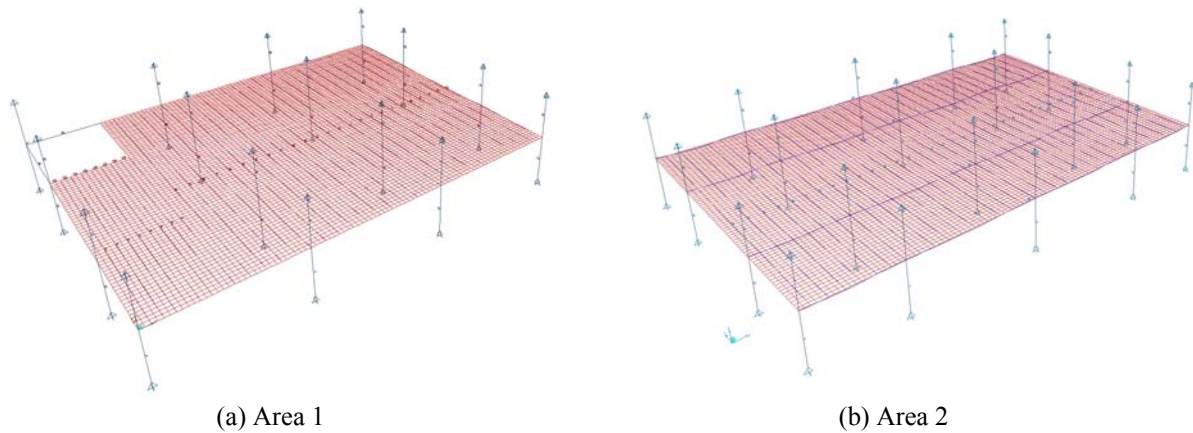


Figure 2.1: Finite Element Model of the Two Areas

The moment demands given in Table were used as a reference for the test setup design. This analysis and the loading layout given resulted in the discovery that an equivalent load  $P_{LL}$  of 20 kips was to be applied at each loading point to reach the ultimate moment of the slab in correspondence with the columns ( $M_u = \phi M_n$ ).

The value for the point load  $P_{LL}$  chosen for the load test was determined to produce the moment at the column's line of interest equivalent to the uniform load applied on the portion of structure under investigation and multiplied by various safety factors. Table 2.2 summarizes the findings

in terms of point load  $P_{LL}$  determined prior to testing using the actual loading configuration for all the tests.

Please note that the equivalent point loads with simulated shear collars are significantly lower than the ones after CFRP strengthening. This result is because the presence of the shoring posts modified the static scheme of the structure as shown in Figure 2.2. The shoring posts acted as an elastic support next to the area where the moments were to be calculated, resulting in much lower loads for those tests in which they were to be used.

Table 2.2: Target Point Load PLL Values

Structural Configuration	Criteria	Code	Load Combination	$P_{LL}$ [kip]
CLT (with collar)	Moment at the outer face of shoring posts (Uniform Direction)	ACI 437	$1.0D_W+1.6L$	11.5
		ACI 318 <sup>(2)</sup>	$1.15D+1.5L$	13.0
24h (with collar)	Moment at the outer face of shoring posts (Uniform Direction)	ACI 318 <sup>(2)</sup>	$1.15D+1.5L$	13.0
CLT (with CFRP strengthening)	Moment at the face of the capital (Uniform Direction)	ACI 437	$1.0D_W+1.6L$	15.0
		ACI 318 <sup>(2)</sup>	$1.15D+1.5L$	17.5
		ACI 318 - C <sup>(3)</sup>	$1.2D_W+1.6L$	19.5

<sup>(1)</sup> Equivalent load PLL was kept constant on the structure for 24 hours; <sup>(2)</sup> Value under consideration by ACI 318;

<sup>(3)</sup> Value Proposed by ACI-318-C

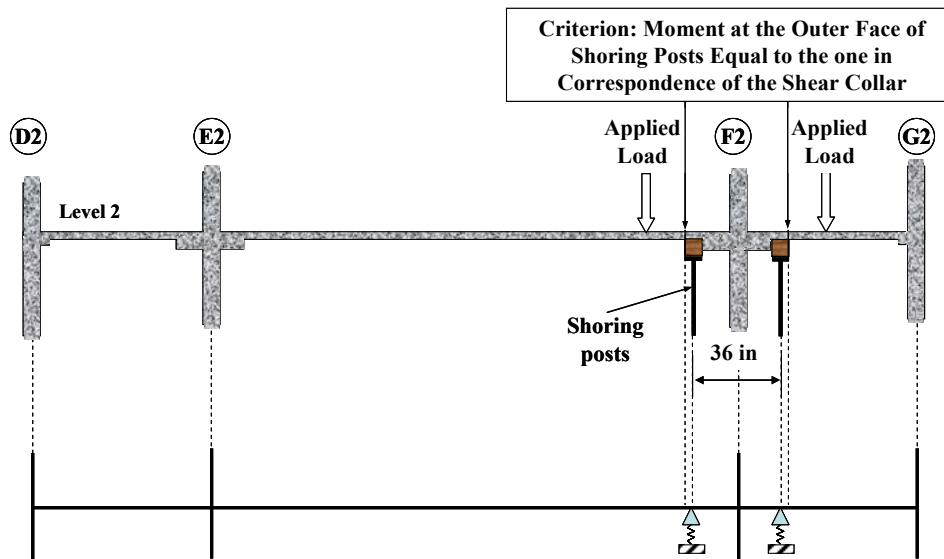


Figure 2.2: Modification of the Static Scheme of the Structure Due to the Installation of the Shoring Posts (Simulated Shear Collars)

## 3 Description of the Load Test

### 3.1 Testing Apparatus

The testing equipment used consists of four 100-ton hydraulic cylinder jacks and a hydraulic pump for applying the load, direct current differential transducers (DCDT's) for measuring deflections, and one 100-kip and one 200-kip load cell for measuring the applied loads (see Figure 3.1). The DCVTs were mounted on tripods supported on the level below the one being tested.

A data acquisition system recorded data at a rate of 1 Hz from all devices, displaying the load-vs.-deflection curves of two significant locations in real time on a computer screen (see Figure 3.2).

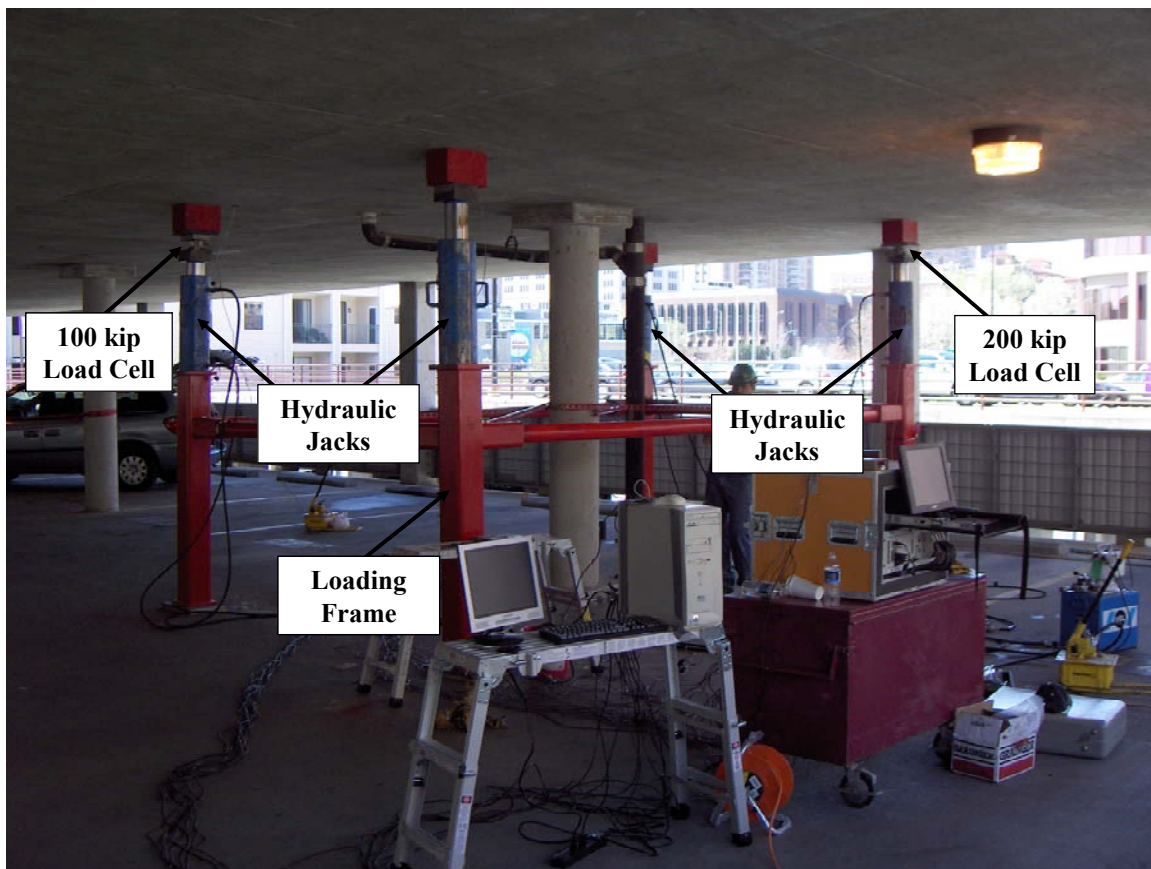


Figure 3.1: Loading and Measuring Equipment

The list of the instruments used is given in Table.1. Note that the strain gages were applied on the FRP laminates after the strengthening.



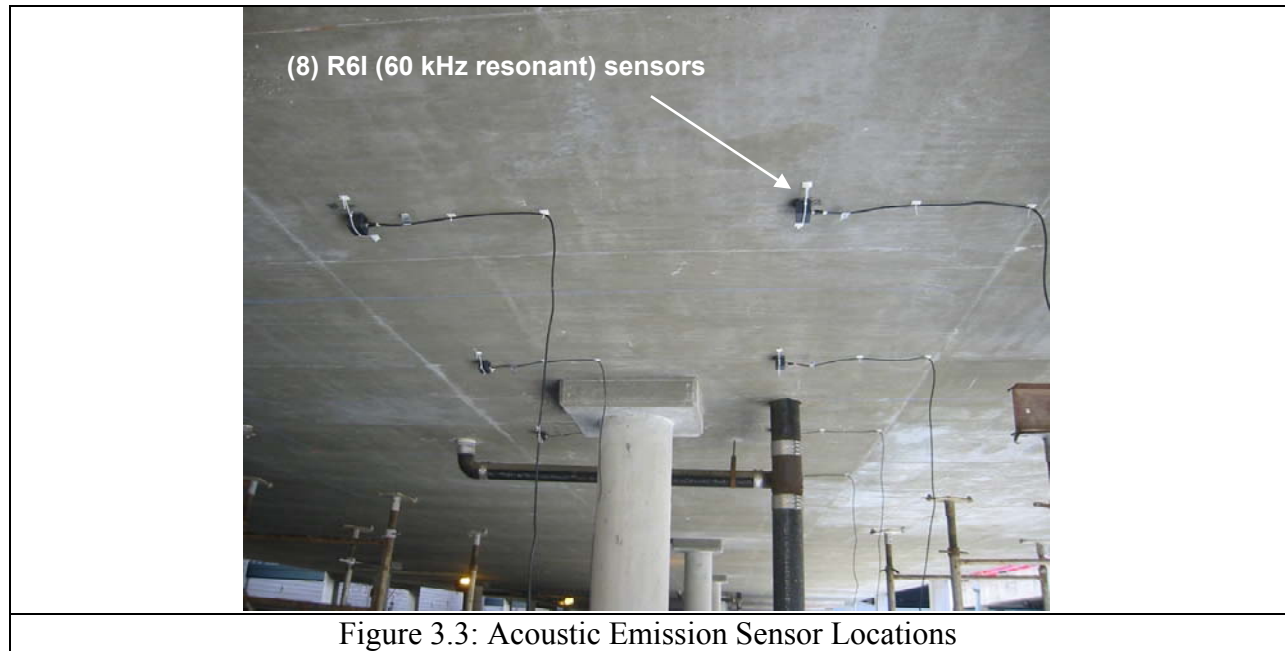
Figure 3.2: Data Acquisition System

Table 3.1: Instrumentation

Code	Channel	Device	Measurement
LC1	1	Load Cell	Applied Load
LC2	2	Load Cell	Applied Load
DS1	3	±0.5 in DCVT	Deflection (Slab)
DS2	4	±0.5 in DCVT	Deflection (Slab)
DS3	5	±0.5 in DCVT	Deflection (Slab)
DS4	6	±0.5 in DCVT	Deflection (Slab)
DS5	7	±0.5 in DCVT	Deflection (Slab)
DS6	8	±0.5 in DCVT	Deflection (Slab)
DS7	9	±1 in DCVT	Deflection (Slab)
DS8	10	±1 in DCVT	Deflection (Slab)
DS9	11	±1 in DCVT	Deflection (Slab)
DS10	12	±2 in DCVT	Deflection (Slab)
DS11	13	±2 in DCVT	Deflection (Slab)
DS12	14	±2 in DCVT	Deflection (Slab)
DS13	15	±2 in DCVT	Crack Opening
DS14	16	±2 in DCVT	Crack Opening
SS1	33	Strain Gage	FRP Laminate
SS2	34	Strain Gage	FRP Laminate
SS3	35	Strain Gage	FRP Laminate
SS4	36	Strain Gage	FRP Laminate
SS5	37	Strain Gage	FRP Laminate
SS6	38	Strain Gage	FRP Laminate
SS7	39	Strain Gage	FRP Laminate
SS8	40	Strain Gage	FRP Laminate

The data acquisition system for Acoustic Emission was a digital DiSP system manufactured by Physical Acoustics Corporation (PAC). This system has 2 high-speed data acquisition boards and is capable of monitoring 8 channels simultaneously. The sensors used were R6I (resonant

sensors with peak frequency in the vicinity of 60 kHz and integral 40 dB preamplifiers) also manufactured by PAC. The sensors were connected to the data acquisition system with co-axial cables approximately 100 feet in length. The sensors were mounted in a grid with outside dimension of 5 feet by 15 feet centered on the column location. This arrangement was determined on-site and was based on the visible crack locations and loading arrangement. Sensors were mounted on the compression face (underside of the slab). The couplant was high vacuum grease. Contact was maintained with specially fabricated sensor hold-down devices. The test threshold varied between 30 dB and 35 dB. The evaluation threshold was in all cases 45 dB. The sensor locations are shown in Figure 3.3.



### 3.2 Load Test Configurations

The load tests were performed in a push-down method. In particular, 4 hydraulic jacks (1 for each loading point) were used to provide the load that resulted in downward concentrated forces on the test member.

Figure shows an overall schematic of the push-down test for the two tested areas. Shoring was installed on one floor above the tested member to provide contrast and to reduce the amount of contrasting weights. Shoring posts were mounted around the column being tested using the configuration shown in the figures to simulate the presence of shear collars and to avoid the shear failure of the slab. Additionally, wood bearing pads were used between the spreader beams and the structural floor to protect the concrete from any localized damage.



### **3.3 Deflection Measurement**

Deflection measurements were taken in 14 different locations, so a significant portion of the floor was monitored during the load test. Deflection measurements were taken with 0.5 in, 1 in, and 2 in DCVTs mounted on tripods on the level below the one being tested. The layout of the DCVTs for the 4 load tests is shown in Figures 3.4 and 3.5.

For the load test after strengthening, a total of eight strain gages were distributed in correspondence with the existing crack injected before strengthening. At these locations the strain on the FRP laminates was expected to be higher, allowing the determination of how the load is distributed between different laminates (Figure 3.6)

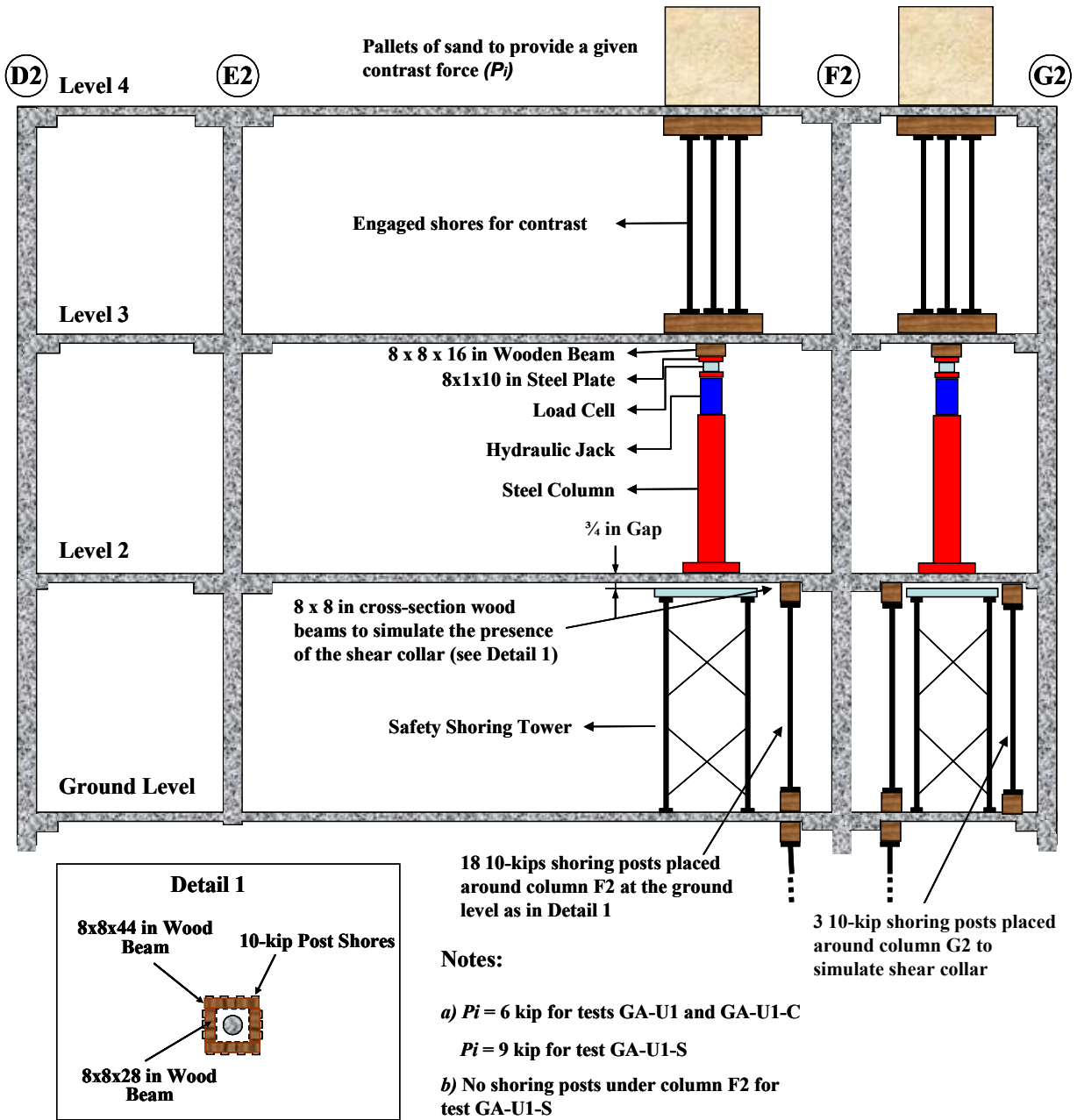


Figure 3.4: Schematic of the Load Tests (with Simulated Shear Collar)

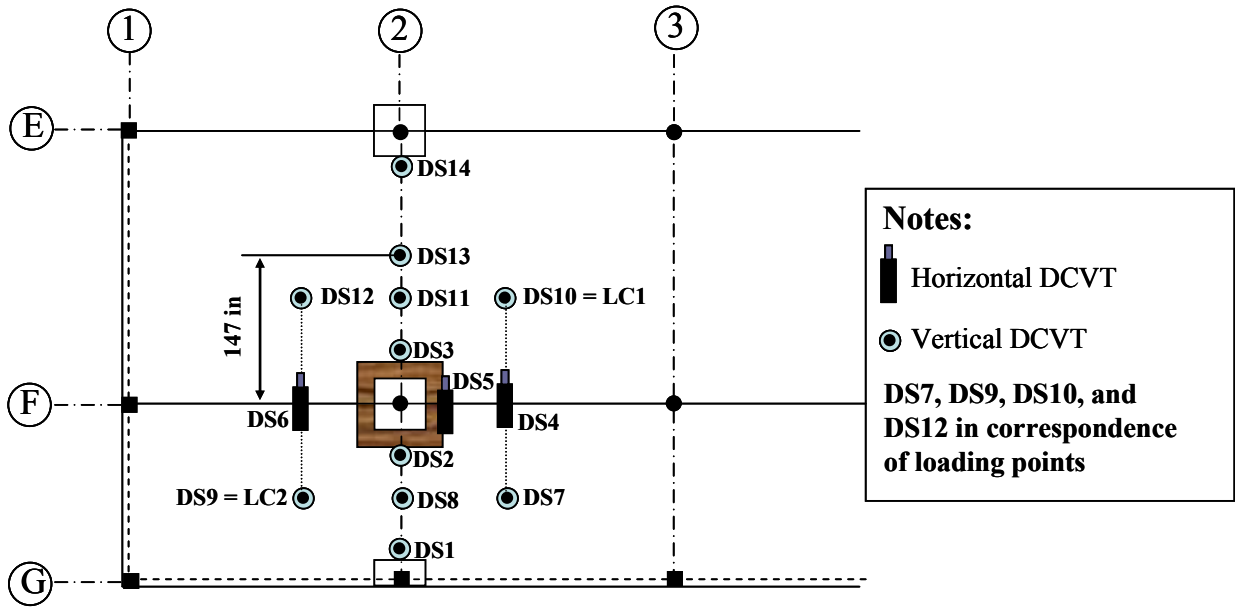


Figure 3.5: Distribution DCVTs (All Load Tests)

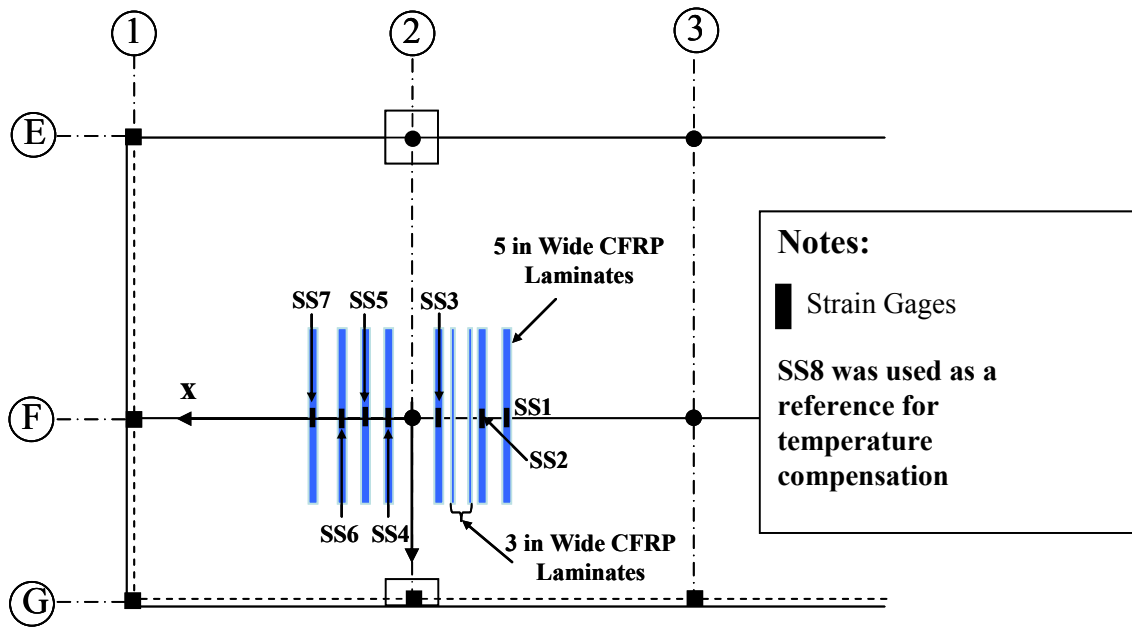


Figure 3.6: Distribution Strain Gages (with CFRP Strengthening)

## 4 Testing Procedure

This section describes the loading procedure used for all the different tests. For all the tested areas, once all instruments were connected, a preliminary load was applied to seat all test setup components and to eliminate slack in the system. Following the preliminary load, the slab was loaded in 8 loading cycles with simulated shear collars (before CFRP strengthening) and 10 cycles after CFRP strengthening. Each load cycle consists of loading the slab in steps. A minimum of 4 approximately equal load steps were used to load the slab, followed by at least 2 steps to unload. Each load step was maintained for at least 2 minutes. During this time the displacement at several locations was monitored for stability. The peak load for each successive cycle was increased to approach the maximum test load. Two cycles using the maximum test load were applied to verify repeatability of the measurements.

Figure 4.1 to Figure 4.3 show the applied load cycles. Please note that the actual load cycles may vary slightly depending on the performance of the system as monitored during the test and the minimum load that has to be maintained to eliminate slack in the system. Also note that the applied load cycles do not start from zero to account for the weight of the testing equipment that was measured to be 800 lb (360 kg) per loading point.

The 24-hour load test was also conducted as prescribed by ACI318-05 and is shown in Figure 4.2.

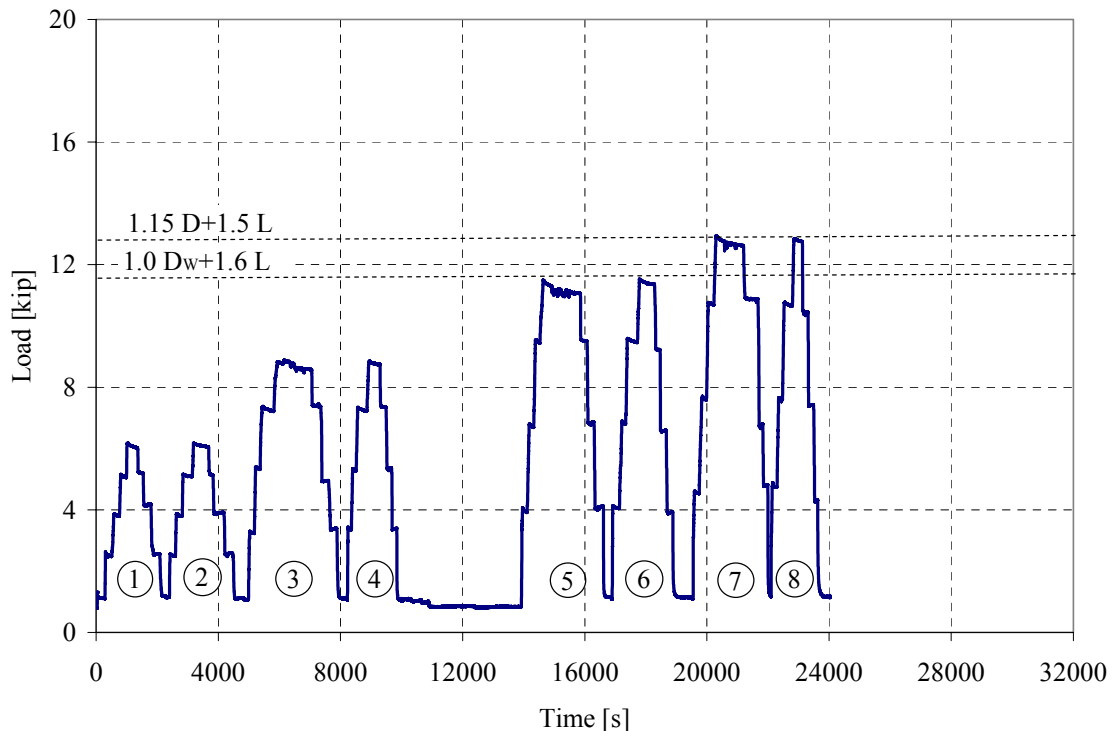


Figure 4.1: Load Cycles (with Simulated Shear Collar)

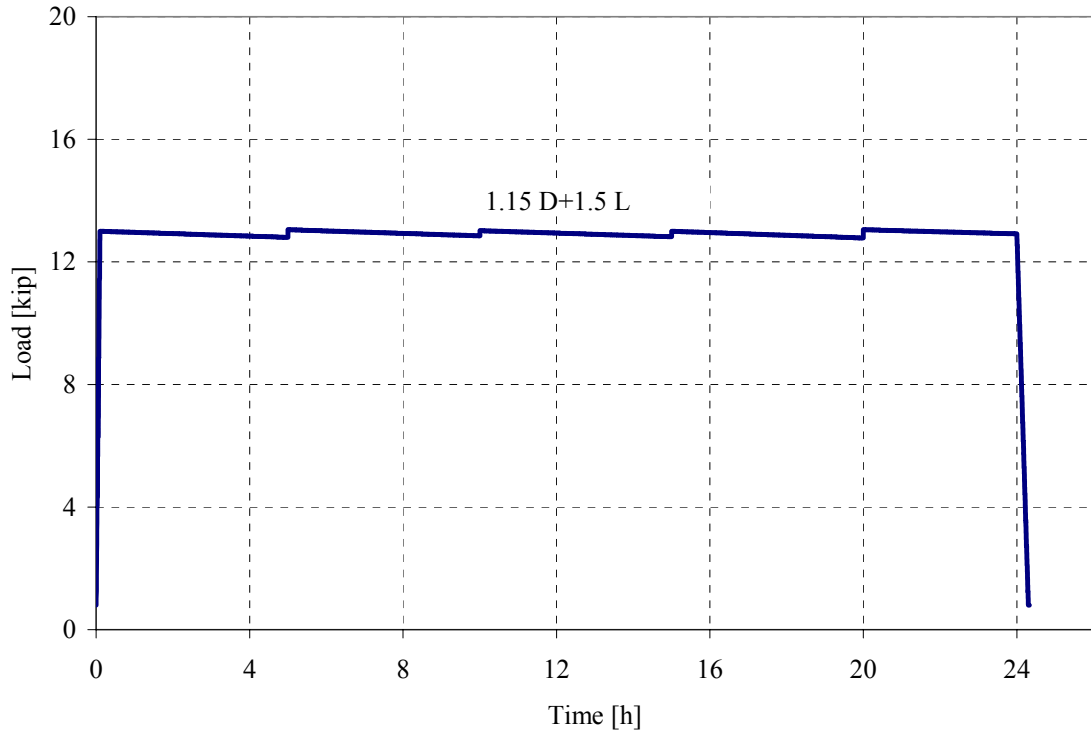


Figure 4.2: 24-h Load Test (with Simulated Shear Collar)

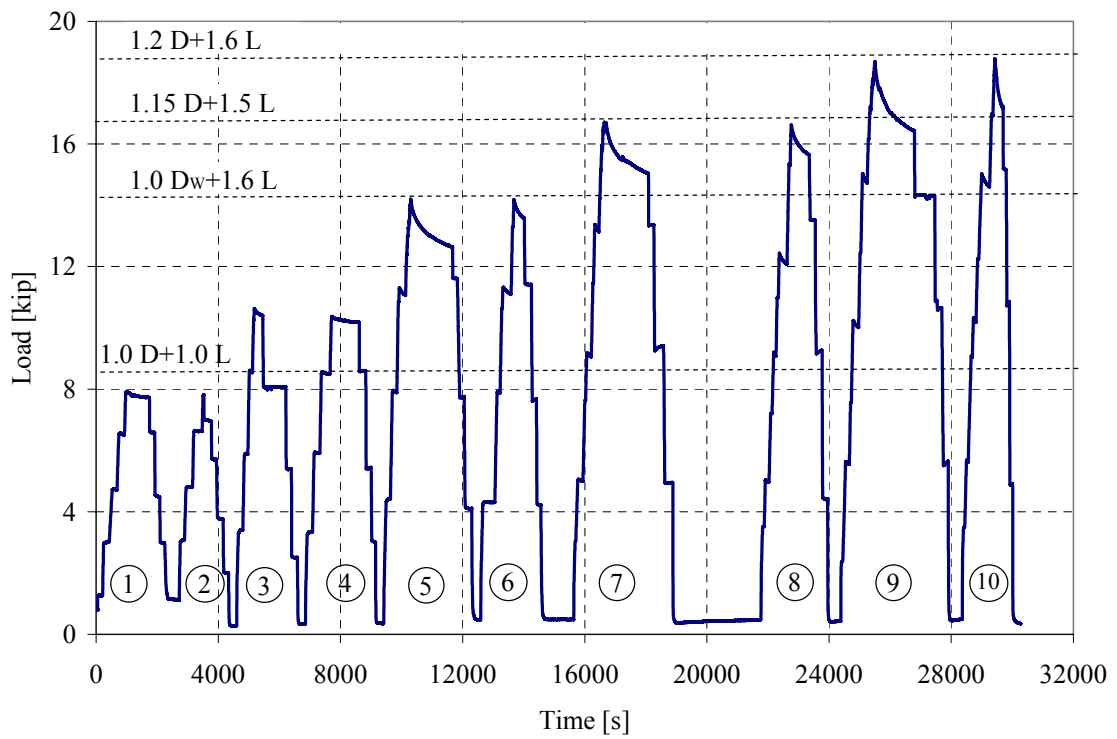


Figure 4.3: Load Cycles (with CFRP Strengthening)

# 5 TEST RESULTS AND DISCUSSION

The following sections describe the results of the four tests for the two areas. Only the measurements from the sensors at the most demanding locations are reported. The other sensors described previously were used for the validation of the finite element models. In all the tests a very good agreement between experimental and finite element models was observed.

## 5.1 Cyclic Load Test (with Simulated Shear Collar)

The structure was loaded using the procedure shown in Figure 5.1. In accordance to ACI 437, the load level for cycles 5 and 6 was at 11.5 kip, while the last 2 cycles were conducted at a load level corresponding to 1.15D+1.5L. No evident failure signs were observed at these load levels. Figure shows the measured deflections by DCVT DS10 during the 8 cycles. As seen in the figure, the behavior of the structure was elastic with no residual deflection measured when the load was removed. The structure passed the test since repeatability, permanency, and deviation from linearity were within the limits prescribed by ACI 437 (See Table 5.1). Note that the deviation from linearity was calculated considering the deflections at the fourth load cycle.

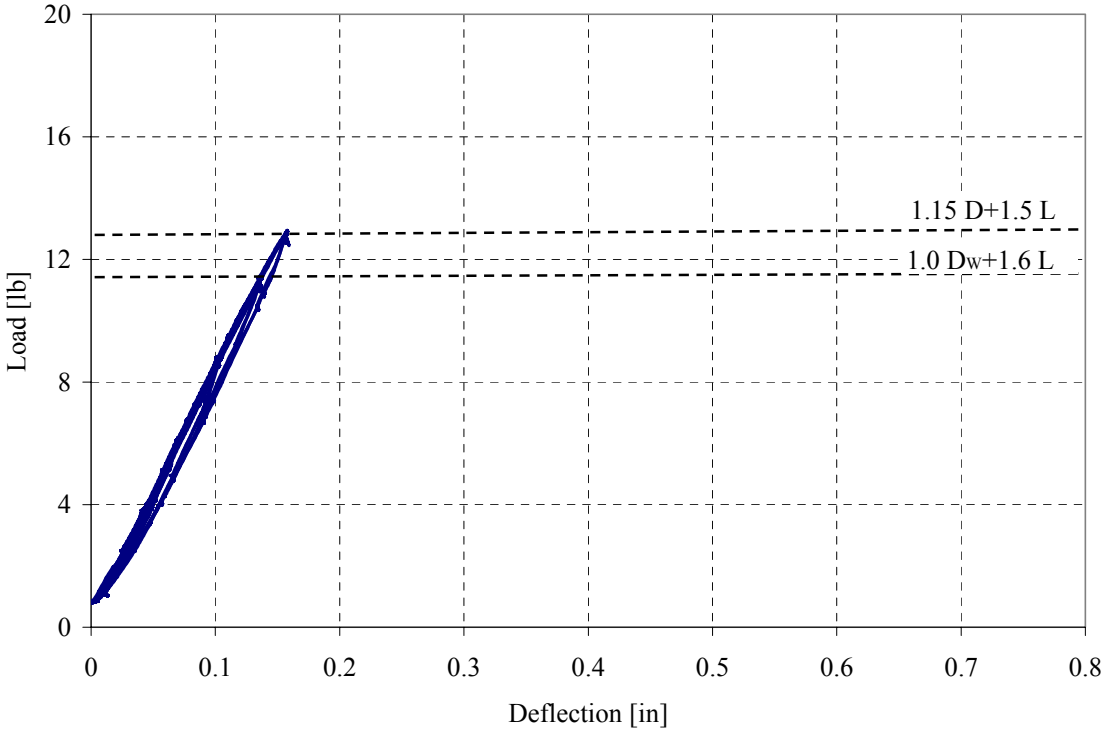


Figure 5.1: Load Deflection Diagram (with Simulated Shear Collar)

No new cracks were observed while performing the cyclic load test; the effect of the applied loads was mostly to increase the size of the existing cracks, as shown in Figure 5.2. The maximum change in width of existing flexural cracks at the service load condition (1.0 D + 1.0

L) was 0.0045 in, and it did not exceed the suggested tolerable crack width of 0.007 in reported by ACI Committee 224 (ACI 224R) for this type of structure and environmental condition.

Table 5.1: Experimental Results (with Simulated Shear Collar)

Load Cycles	Load Level	Repeatability ( $\geq 95\%$ ) (%)	Permanency ( $\leq 10\%$ ) (%)	Deviation from Linearity ( $\leq 25\%$ ) (%)	Performance
1 and 2	0.5(1.0D <sub>w</sub> +1.6L)	103.9	2.1	0.3	Satisfactory
3 and 4	0.75(1.0D <sub>w</sub> +1.6L)	102.1	3.3	0.5	Satisfactory
4 and 6	1.0D <sub>w</sub> +1.6L	101.7	4.0	NA	Satisfactory
7 and 8	1.15D+1.5L	101.2	7.2	NA	Satisfactory

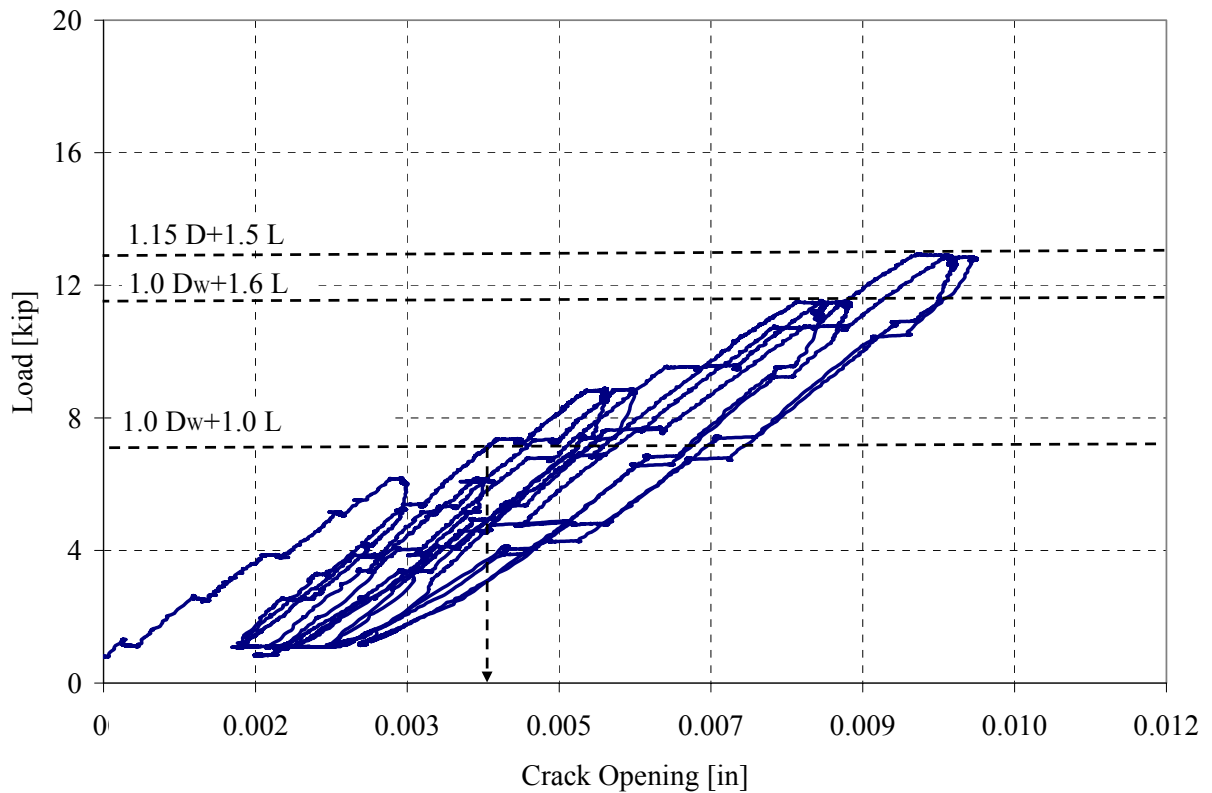


Figure 5.2: Crack Opening Measured by DCVT DS4 (with Simulated Shear Collar)

## 5.2 Acoustic Emission (with Simulated Shear Collar)

The results of this evaluation procedure are shown in Figure 5.3a through 5.3c. The figures address results for the cumulative signal strength ratio, the Felicity ratio, and the Calm ratio vs. Load Ratio, respectively.

### **Cumulative signal strength ratio**

The results of this evaluation procedure are shown in Figure 5.3a. In this figure the value of CSS for loading of both cycles of each loadset are shown as bar graphs (for example, loadset 4a represents loadset 4, cycle 1). The CSS ratio is shown above the bar graph for the reload cycle. The limited studies by Ridge indicated that CSS ratios in excess of 40% were indicative of a severe level of damage. The values shown in Figure 3a are less than this value in all cases.

### **Felicity ratio**

The results of the Felicity ratio for each reloading phase are shown in Figure 5.3b. The Felicity ratio does decrease with increased loading but is never less than 0.90.

### **Calm ratio versus load ratio (Felicity ratio)**

The calm ratio was calculated for the reloading cycles only. The results are plotted graphically in Figure 5.3c. The reloading cycles 2b, 3b, and 4b fall within the same general range.



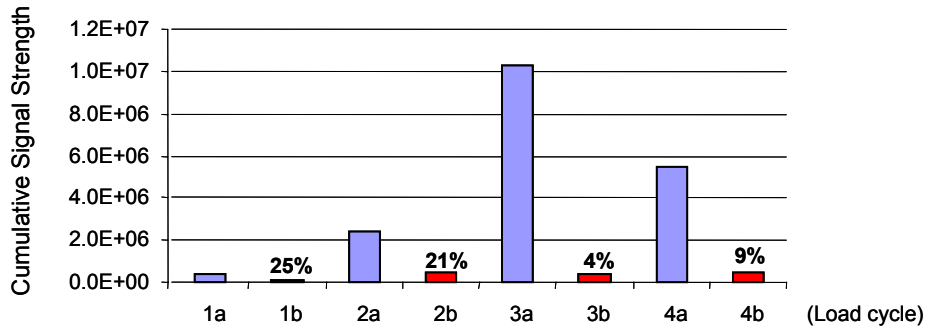


Figure 5.3a: Cumulative Signal Strength Ratio Results (with Simulated Shear Collar)

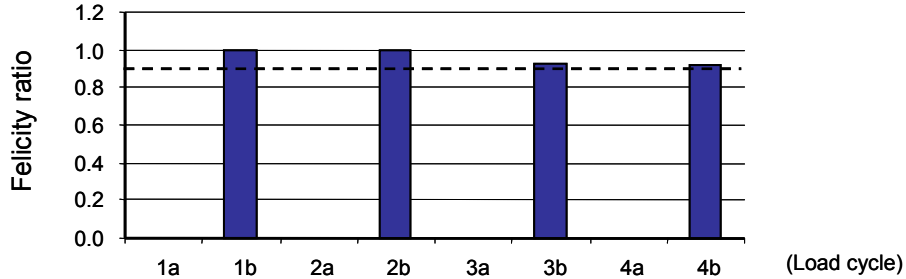


Figure 5.3b: Felicity Ratio Results (with Simulated Shear Collar)

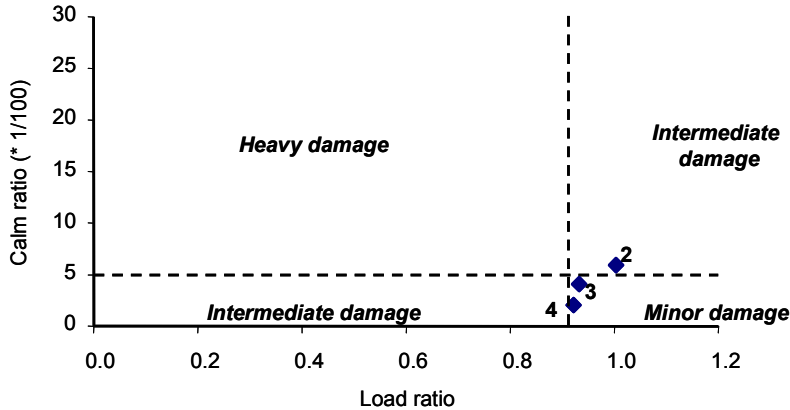


Figure 5.3c: Calm vs. Load Ratio Results (with Simulated Shear Collar)

### 5.3 24-h Load Test (with Simulated Shear Collar)

After concluding the cyclic load, the maximum load reached was kept on the structure for 24 hours. Figure 5.4 shows the corresponding time-deflection diagram.

The structure also met the criteria of Chapter 20 of ACI 318-05, since at the completion of the 24-hour duration under maximum load and upon unloading, the two criteria listed below were verified:

$$\Delta_{max} = \Delta_{max,24h} + \Delta_{r,cyclic} = 0.18 \text{ in} + 0.01 \text{ in} = 0.19 \text{ in} \leq \frac{l_t^2}{20,000h} = 0.79 \text{ in} \quad (1)$$

and

$$\Delta_{r,max} = \Delta_{r,max,24h} + \Delta_{r,cyclic} = 0.019 \text{ in} + 0.01 \text{ in} = 0.029 \leq \frac{\Delta_{max}}{4} = 0.045 \text{ in} \quad (2)$$

where  $\Delta_{r,cyclic}$  is the residual deflection after the cyclic load test and  $\Delta_{max,24h}$  and  $\Delta_{r,max,24h}$  represent the maximum and the residual deflection after the 24-hour load test, respectively. Equations (1) and (2) account for the fact that the 24-hour test was conducted following the cyclic load test and, therefore, the computation of both maximum and residual deflections had to account for the residual deflection of the cyclic load test.

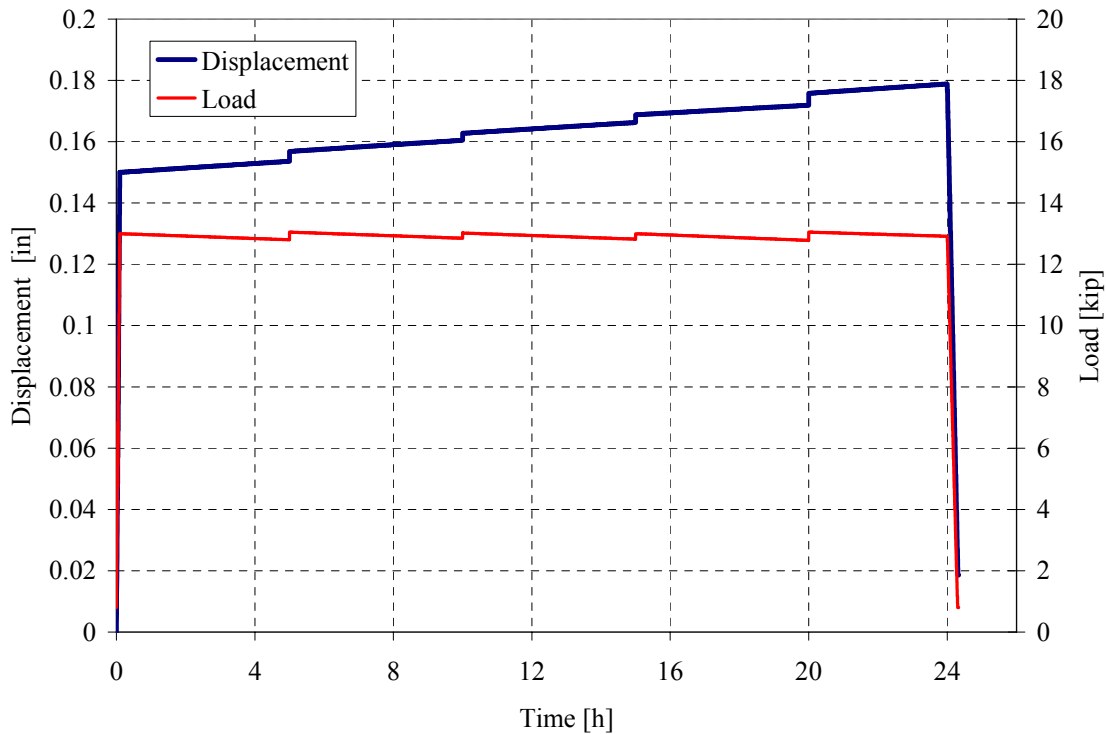


Figure 5.4: Time Deflection Diagram for the 24-Hour Load Test (with Simulated Shear Collar)

#### 5.4 Cyclic Load Test (with CFRP Strengthening)

The structure was loaded using the procedure shown previously. In accordance with ACI 437, the load level for cycles 5 and 6 was at 15 kip; cycles 7 and 8 were conducted at a load level corresponding to 1.15 D + 1.5 L, and the last two cycles at the design load level. No evident failure signs were observed at these load levels. The major effect of the applied load was to reopen the flexural crack injected prior to strengthening. Figure 5.5 shows the measured deflections by DCVT DS10 during the 10 cycles. No cracking signs were observed up to a load level of 10 kip. At this load level, the flexural crack injected prior to strengthening reopened causing significant permanent deflection upon unloading. For this reason, the slab did not meet the criteria prescribed by ACI 437 as shown in Table 5.2. The acceptance criterion of 10 percent

prescribed by ACI 437 is very conservative based on the evidence provided by Bares and FitzSimons [1975] showing that a 20 percent permanency for PC structures is common.

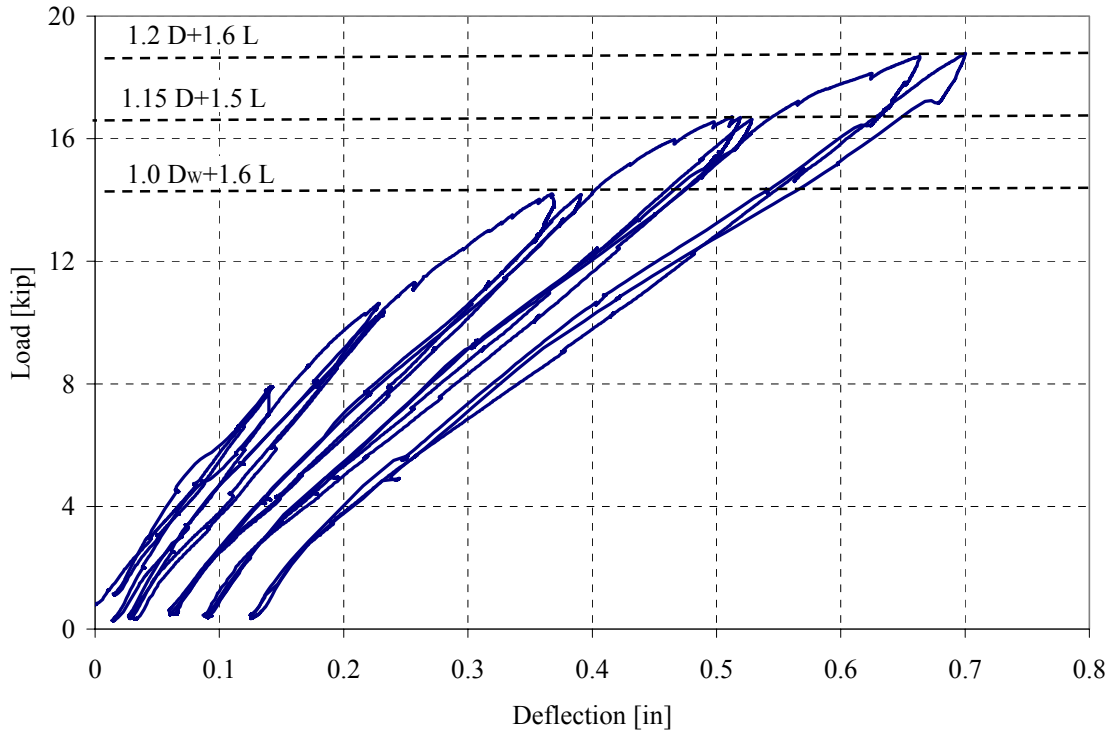


Figure 5.5: Load Deflection Diagram Test GA-U1-S

The structure strengthened with CFRP has a lower stiffness than the one retrofitted with shear collars simulated with shear posts. This fact is also because the presence of the shoring posts modified the static scheme of the structure.

Once the crack opened, the maximum change in width of the flexural cracks at the service load condition was 0.0042 in, and it did not exceed the suggested tolerable crack width of 0.0070 in reported by ACI Committee 224 (ACI 224R) for this type of structure and environmental condition (see Figure 5.6)

Table 1.2: Experimental Results Test (After CFRP Strengthening)

Load Cycles	Load Level	Repeatability ( $\geq 95\%$ ) (%)	Permanency ( $\leq 10\%$ ) (%)	Deviation from Linearity ( $\leq 25\%$ ) (%)	Performance
1 and 2	0.5(1.0D <sub>w</sub> +1.6L)	108.7	9.6	3.5	Satisfactory
3 and 4	0.75(1.0D <sub>w</sub> +1.6L)	106.4	<b>11.9</b>	10.4	Unsatisfactory
5 and 6	1.0D <sub>w</sub> +1.6L	105.3	<b>16.4</b>	NA	Unsatisfactory
7 and 8	1.15D+1.5L	103.2	<b>17.5</b>	NA	Unsatisfactory
9 and 10	1.2D+1.6L)	98.6	<b>17.5</b>	NA	Unsatisfactory

Figure 5.7 shows the distribution of strain as a function of the applied load. The figure shows that the crack likely started opening from the side of strain gage SS1 and propagated to the other side of the column. When close to the ultimate load, the strain tends to become uniform between all instrumented FRP strips as assumed in the design. A significant residual strain was recorded after unloading because of the inability of the crack to completely close. No signs of CFRP delamination were observed during the test (see Figure 5.8Figure ).

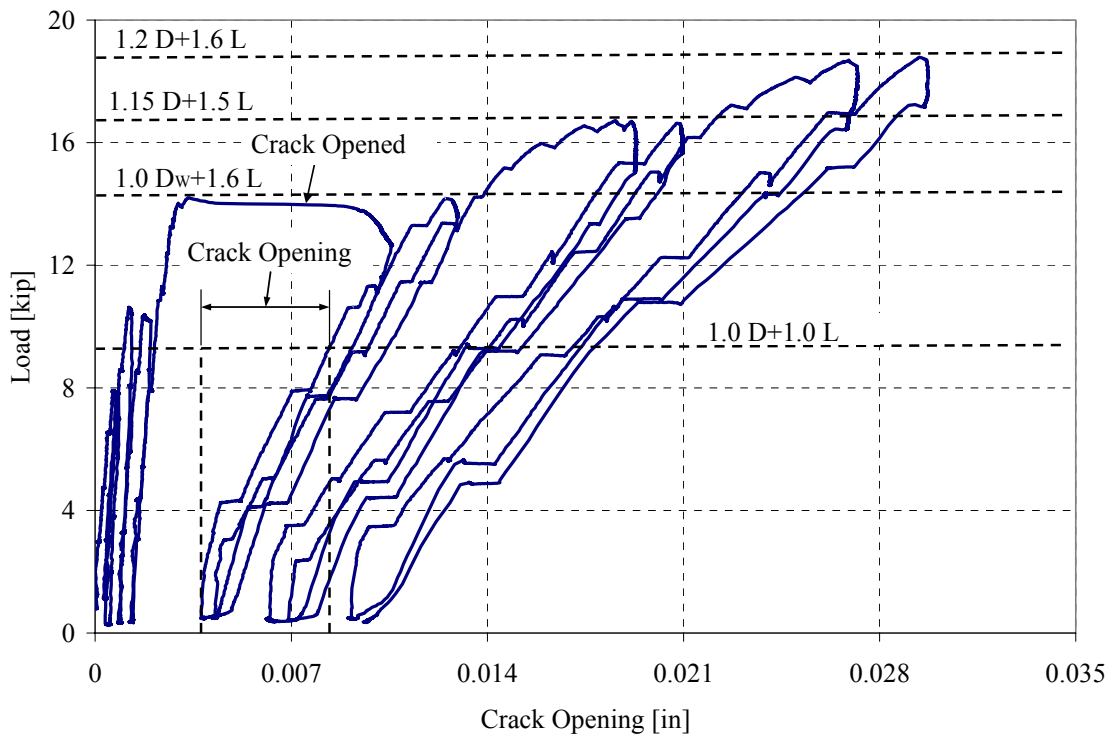


Figure 5.6: Crack Opening Measured by DCVT 8 (after CFRP Strengthening)

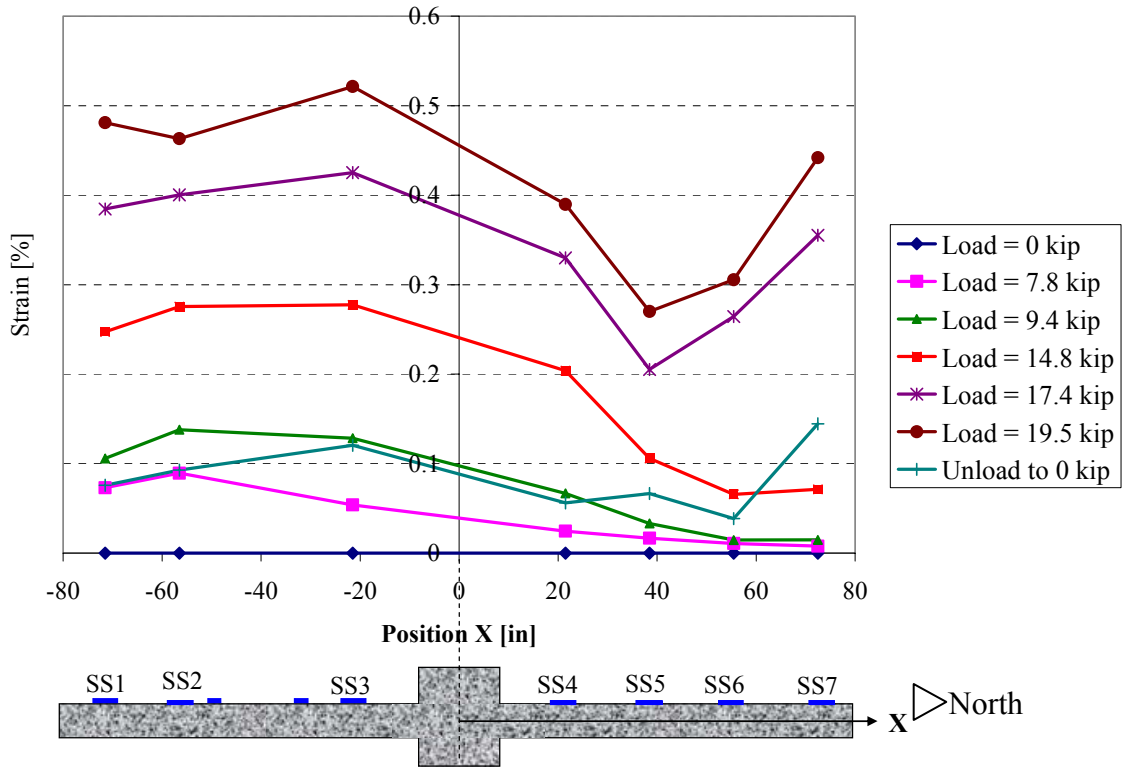


Figure 5.7: Strain Distribution in the FRP (after CFRP Strengthening)



Figure 5.8: CFRP Strengthening Subjected to the Design Load

## **5.5 Acoustic Emission (with CFRP Strengthening)**

The results of this evaluation procedure are shown in Figure 5.9a through 5.9c. As previously figures a through c address results for the cumulative signal strength ratio, the Felicity ratio, and the Calm ratio vs. Load Ratio, respectively.

### **Cumulative signal strength ratio**

The results of this evaluation procedure are shown in Figure 5.9a. The limited studies by Ridge and Ziehl, 2004 indicated that CSS ratios in excess of 40% were indicative of a severe level of damage. The values shown in Figure 3a are less than this value in all cases. However, loadset 5 approaches this value.

### **Felicity ratio**

The results of the Felicity ratio for each reloading phase are shown in Figure 5.9b. The Felicity ratio decreased with increased loading and was first less than 0.90 for reload cycle 2b.

### **Calm ratio versus load ratio (Felicity ratio)**

The calm ratio was calculated for the reloading cycles only. The results are plotted graphically in Figure 5.9c. The reloading cycles 1b, 2b, 3b, and 4b fall within the same general range. Reloading cycle 5b is notable for its significant increase in the calm ratio value.

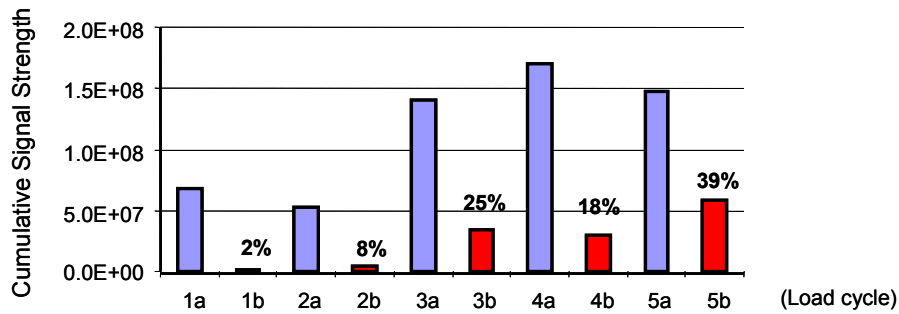


Figure 5.9a: Cumulative Signal Strength Results (with CFRP Strengthening)

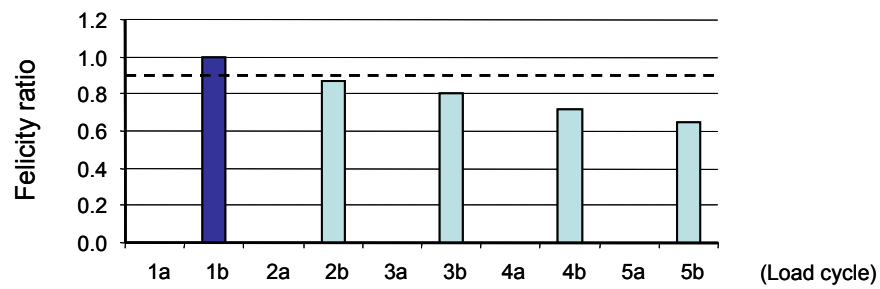


Figure 5.9b: Felicity Ratio Results (with CFRP Strengthening)

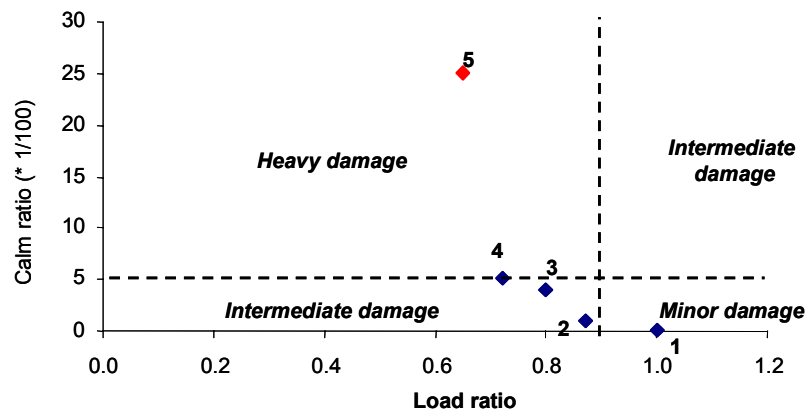


Figure 5.9c: Calm vs. Load Ratio Results (with CFRP Strengthening)

### Location Plot

As mentioned above, source location is not the focus of this investigation. However, it is useful to mention that crack growth during loading can be located rather easily if the wavespeed of the structure is known. Figure 5.10 demonstrates the results of an AE source location plot during reloading.

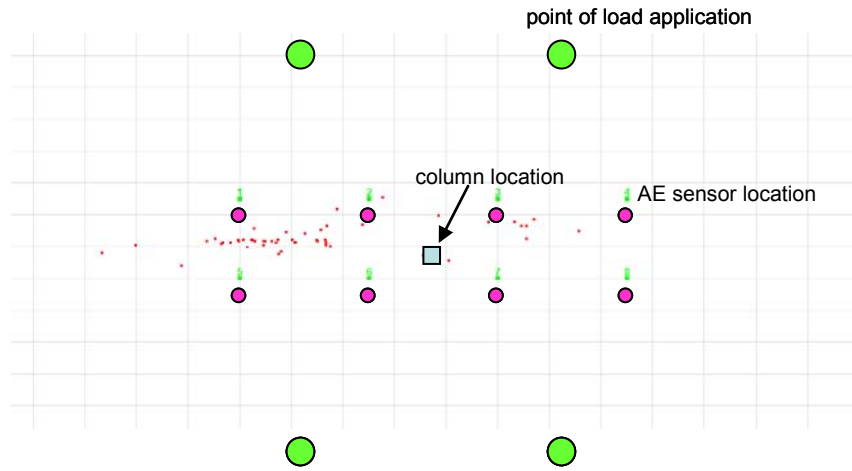


Figure 5.10: Example of AE Source Location



## 6 Conclusions

Two cyclic and one 24-hour load test were performed on the floor system of a parking garage in Kansas City, Missouri. In all load tests, the critical cross-section of interest was in the negative moment region at the column location in correspondence with the capital/shear collar. The three tests were performed at load levels producing the moment at the section of interest equivalent to the uniform load applied on the portion of structure under investigation.

When tested simulating the presence of the shear collar with shoring posts, the structure passed the cyclic load test since repeatability, permanency, and deviation from linearity were within the limits prescribed by ACI 437. The structure also met serviceability criteria since the maximum change in width of existing flexural cracks at the service load condition (1.0 D + 1.0 L) was 0.0045 in, and it did not exceed the suggested tolerable crack width of 0.007 in reported by ACI Committee 224 (ACI 224R) for this type of structure and environmental condition. All of the acoustic emission evaluation criteria were also passed.

In addition to the protocol prescribed by ACI 437, the applied load was kept on the structure for 24 hours as per ACI 318 Chapter 20. The structure also met the latter criteria.

After strengthening with CFRP, the tested area of the structure did not meet the acceptance criterion on permanency prescribed by ACI 437. The acceptance criterion of 10% prescribed by ACI 437 may be conservative based on the evidence provided by Bares and FitzSimons (1975) showing that a 20% permanency for PC structures is common. The acoustic emission criteria were generally passed with the exception of loadset 5 which exhibited 'heavy damage' on the Calm vs. Load ratio plot. The Felicity ratio was less than 0.90 for loadsets 2 through 5.

Further investigations are ongoing related to three AASHTO type III prestressed girders in the structures laboratory at U. South Carolina (Figure 6.1). More definitive conclusions regarding the different loading procedures and evaluation criteria will be drawn at the conclusion of that testing program.



Figure 6.1: AASHTO Type III Prestressed Girder

## **7 ACKNOWLEDGEMENTS**

The authors would like to acknowledge the support of the ACI Concrete Research Council and the very significant technical contributions and guidance of Dr. Antonio Nanni of U. Miami and Dr. Gustavo Tumialan of SGH. The authors would also like to acknowledge the contributions of Paolo Casadei (formerly with U. Bath).



Figure 6.1: AASHTO Type III Prestressed Girder

## 8 REFERENCES

- ACI 224R-01, (2001), "Control of Cracking in Concrete Structures," *American Concrete Institute*, Farmington Hills, MI, pp. 46.
- ACI 318-05, (2005), "Building Code Requirements for Structural Concrete and Commentary (318R-05)," *American Concrete Institute*, Farmington Hills, MI, pp. 443.
- ACI Committee 437, (2006), "Test Load Magnitude," Protocol and Acceptance Criteria, ACI 437-2R-06, *American Concrete Institute*, Farmington Hills, MI, 2006, 83 pp.
- ACI Committee 437, (2004), "Strength Evaluation of Existing Concrete Buildings," ACI 437R-03, *Manual of Concrete Practice*, *American Concrete Institute*, Farmington Hills, MI, 28 pp.
- ASME Section V, (2004a). "Section V - Nondestructive Examination", *American Society of Mechanical Engineers Boiler and Pressure Vessel Code*, New York, New York.
- ASME Section X, (2004b). "Section X - Fiber-Reinforced Plastic Pressure Vessels", *American Society of Mechanical Engineers Boiler and Pressure Vessel Code*, New York, New York.
- ASTM E 1316-06a, (2006), "Standard Terminology for Nondestructive Examinations", *American Society of Testing and Materials*, West Conshohocken, Pennsylvania.
- Bares, R. and FitzSimons, N., (1975), "Load Tests of Building Structures," *Journal of the Structural Division, American Society of Civil Engineers*, Vol. 101, No. ST5, May, pp. 1111-1123.
- Colombo, S., Forde, M., Main, I., and Shigeishi, M., (2005), "Predicting the Ultimate Bending Capacity of Concrete Beams from the 'Relaxation Ratio' Analysis of AE Signals", *Construction and Building Materials*, Vol. 19, pp. 746-754.
- JSNDI (2000) "Recommended Practice for In Situ Monitoring of Concrete Structures by Acoustic Emission", *Japanese Society for Nondestructive Inspection, NDIS 2421*, 6 pp.
- Galati, N., and Nanni, A., (2006), "Load Testing of Two Post-Tensioned Concrete Slabs at Garage A, Windsor on the Plaza, Kansas City, MO – Final Report", *Center for Infrastructure and Engineering Studies, University of Missouri-Rolla*.
- Hearn, S., and Shield, C. (1997) "Acoustic emission monitoring as a nondestructive testing technique in reinforced concrete", *ACI Materials Journal*, Vol. 94, no. 6, pp. 510-519.
- Mettemeyer, M., (1999), "In Situ Rapid Load Testing of Concrete Structures", *Master Thesis, Department of Civil Engineering, University of Missouri-Rolla, Rolla, Missouri, December*.

Ohtsu, M., Uchida, M., Okamoto, T., and Yuyama, S., (2002) "Damage Assessment of Reinforced Concrete Beams Qualified by Acoustic Emission", *ACI Structural Journal*, Vol. 99, No. 4, July-August 2002, pp. 411- 417.

Ridge., A., and Ziehl, P., (2006), "Nondestructive Evaluation of Strengthened RC Beams: Cyclic Load Test and Acoustic Emission Methods", *ACI Structural Journal*, Vol. 103, No. 6, pp. 832-841.

Ziehl, P., (2003a). "Superload Moves Safely over Bonnet Carre' Spillway in Louisiana", *PCI Journal*, Vol 48, No. 5, p. 125.

Ziehl, P., Engelhardt, M., and Schell, E., (2005a). "San Patricio County FRP Bridge – Monitoring Phase One (May 19, 20, and 21, 2004)", *prepared for the Texas Department of Transportation*, Austin, Texas, 54 pp.

Ziehl, P., Engelhardt, M., and Schell, E., (2005b). "San Patricio County FRP Bridge – Monitoring Phase Two (March 3 and 4, 2005)", *prepared for the Texas Department of Transportation*, Austin, Texas, 34 pp.